SAND2022-13470C

In-situ Investigation of Amorphization and Microstructural Changes in $LiAlO_2$

N. Madden, R. Schoell ,E.J. Lang, K. Hattar

Sandia National Laboratories

September 2022

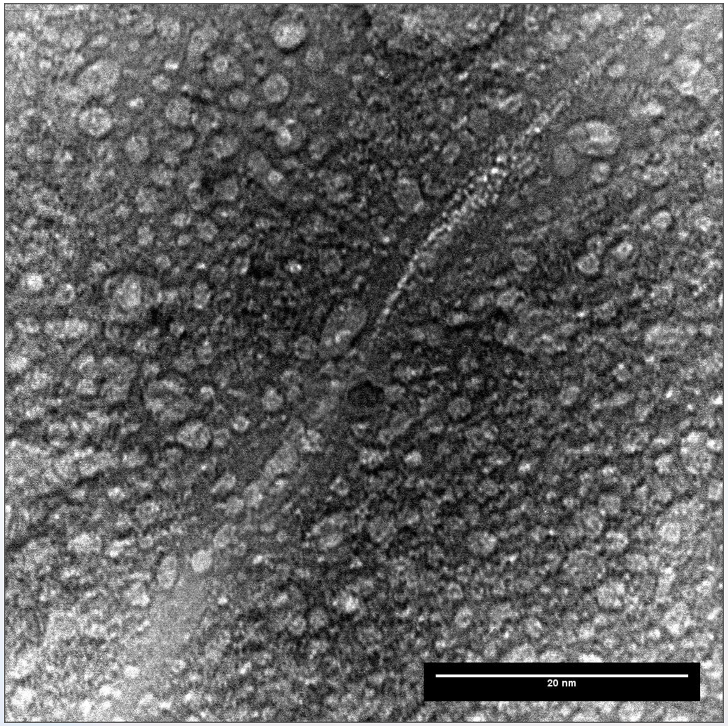

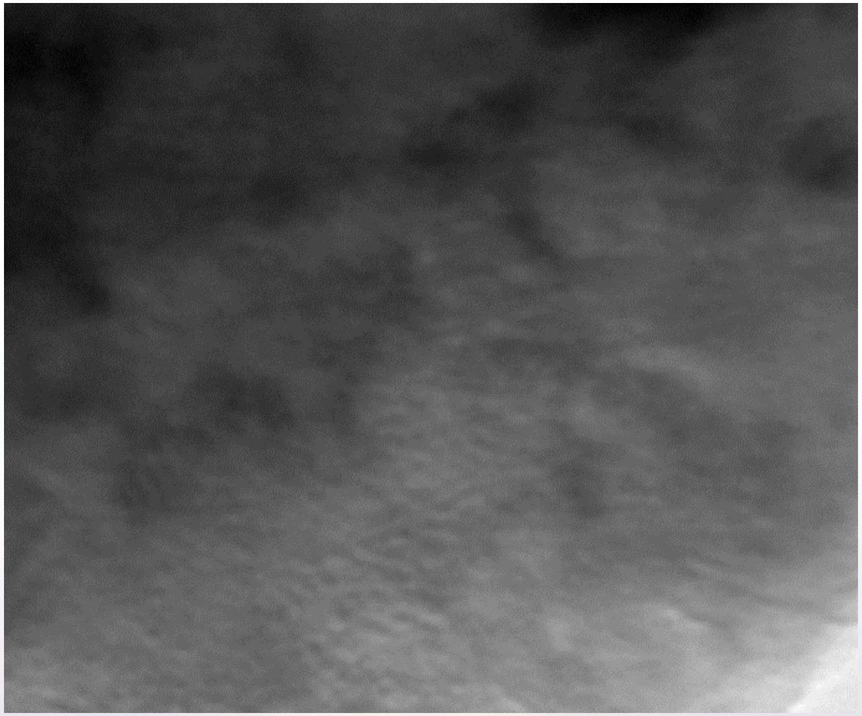

Utilizing *In situ* TEM microscopy to deconvolute governing environments and elucidate the underlying mechanisms.

TPBAR Design & Reactor Environment

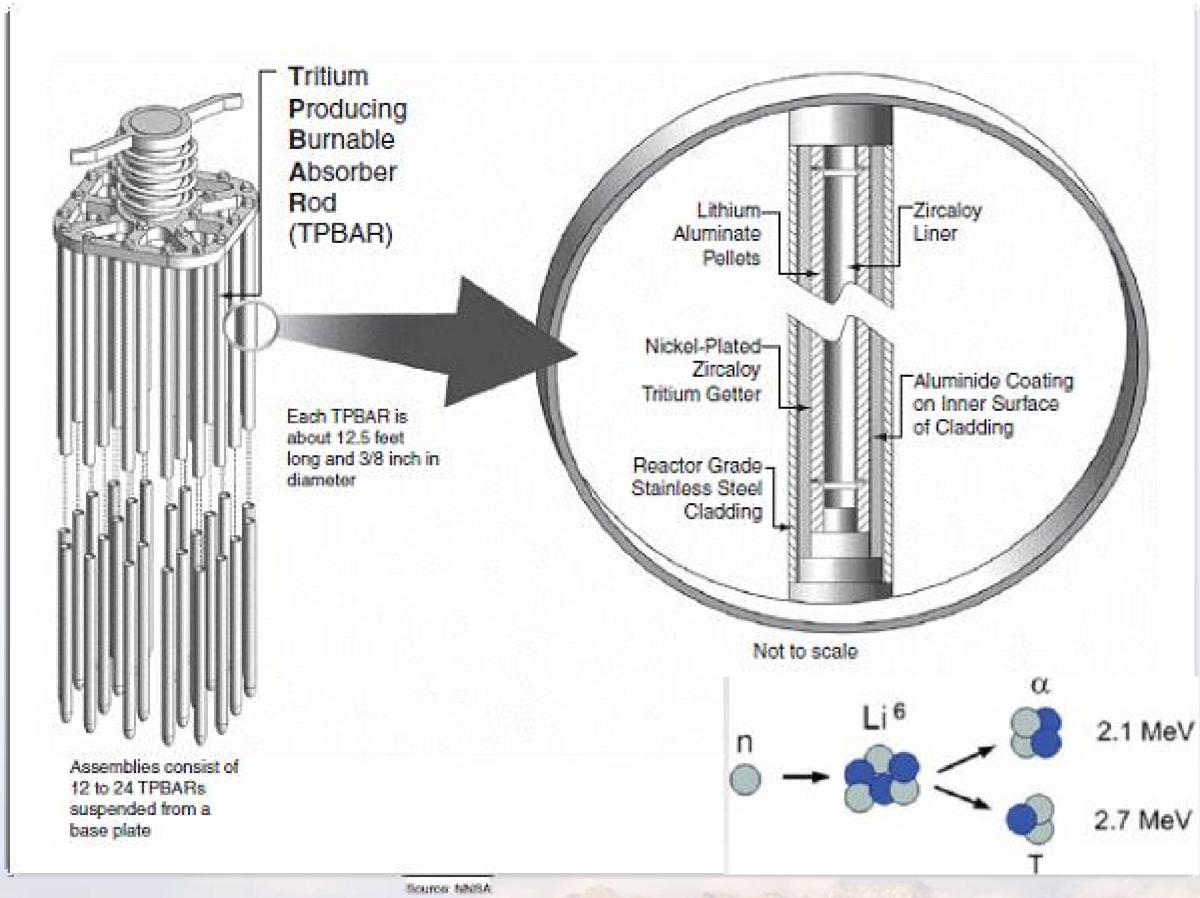

Tritium Producing Burnable Absorber Rod (TPBAR)

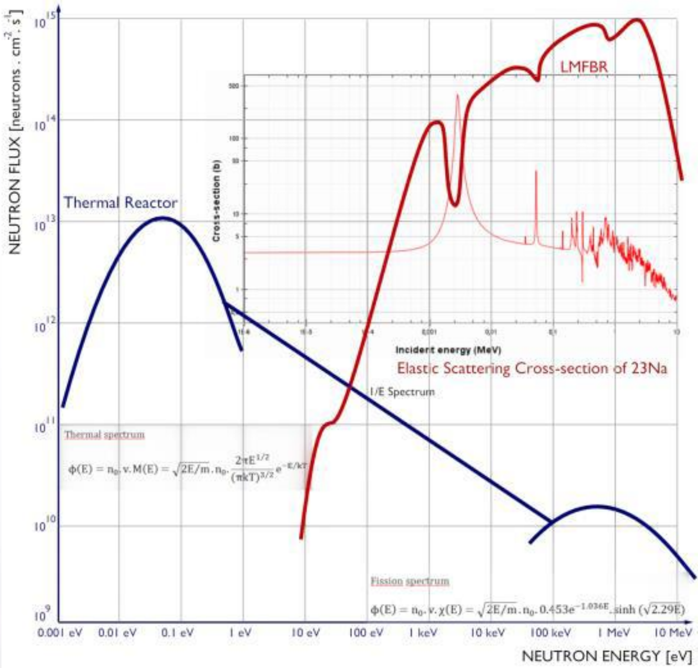

Extremely Complex Environment: Displacement Damage, Tritium Production, Helium Production, Mechanical Stress & Elevated Temperatures

Understanding Tritium Permeation in TPBAR

- **TPBAR ^3H permeation is higher than predictive performance models**
  - In 2004, during Cycle 6, the predicted levels were ~0.5 Ci/TPBAR/cycle and actual levels were ~4 Ci/TPBAR/cycle (0.04% of total ^3H produced)
- **Mechanisms responsible for differences between predictions and observations are not well understood**
- **Currently building an understanding of fundamental ^3H-He-defect interactions**

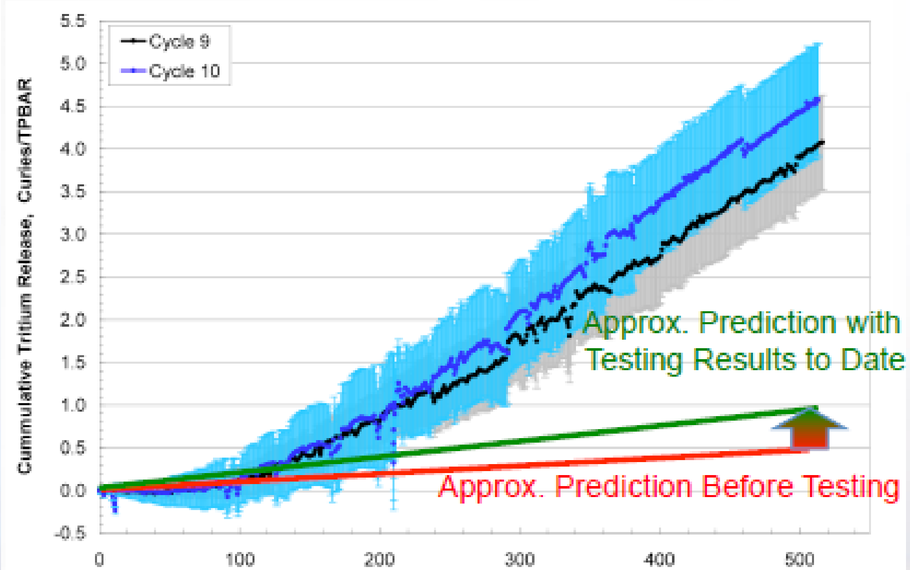

Burkes, et al. TFG Meeting 2016

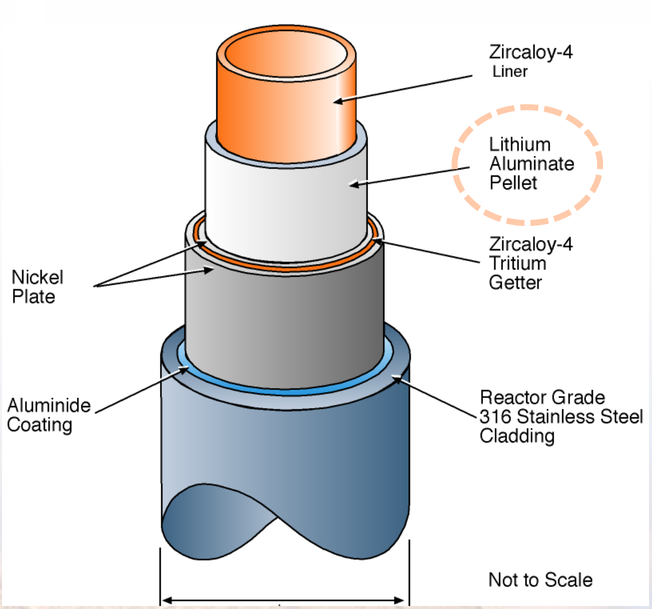

Simulating neutron irradiation in a reactor is complicated, and TPBAR adds the complication of ^3H production

Investigating the nm Scale to Understand the km Scale

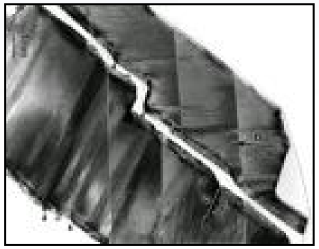

1 nm | 1 μm | 1 mm | 1 m | 1 km | 10^7 m

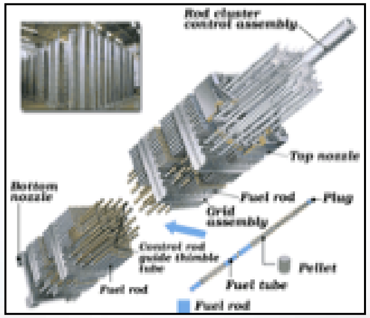

In situ Ion Irradiation TEM (I^3TEM)

Ion Beam Lab (IBL)

Sandia's Ion Beam Laboratory

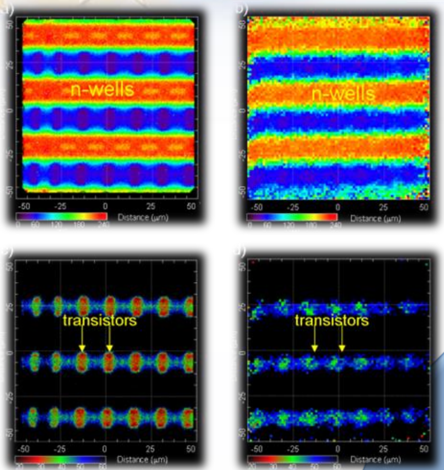

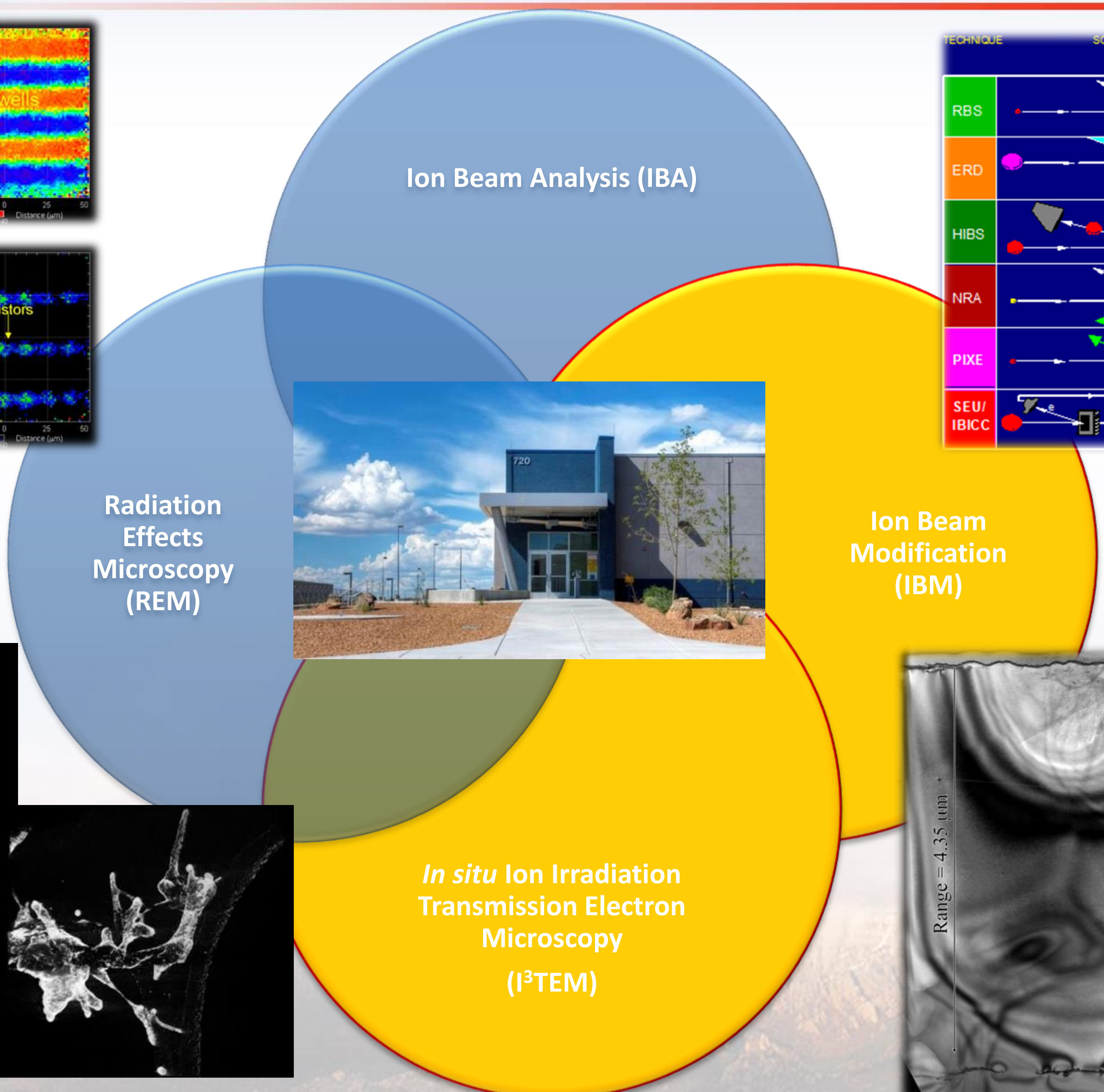

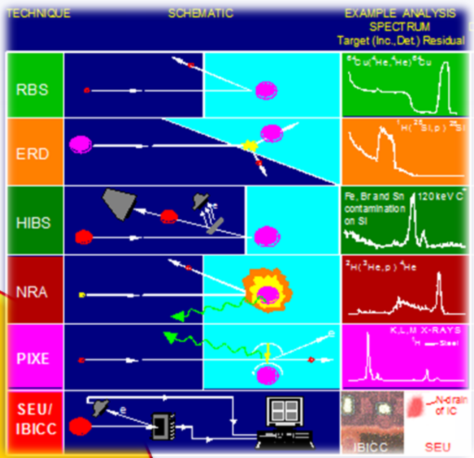

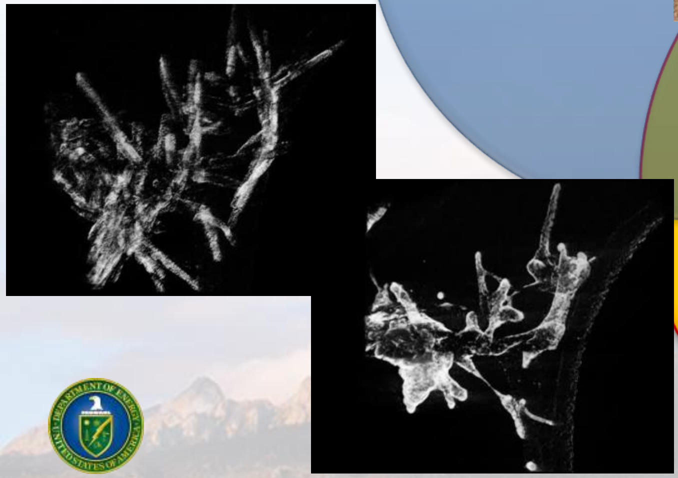

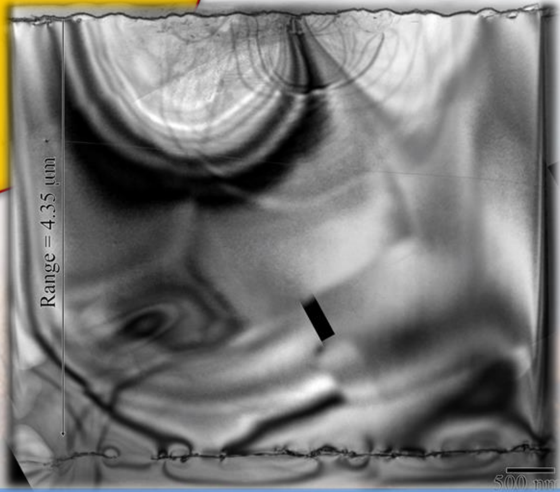

Sandia's Concurrent *In situ* Ion Irradiation TEM Facility

Collaborator: D.L. Buller

IBIL from a quartz stage inside the TEM

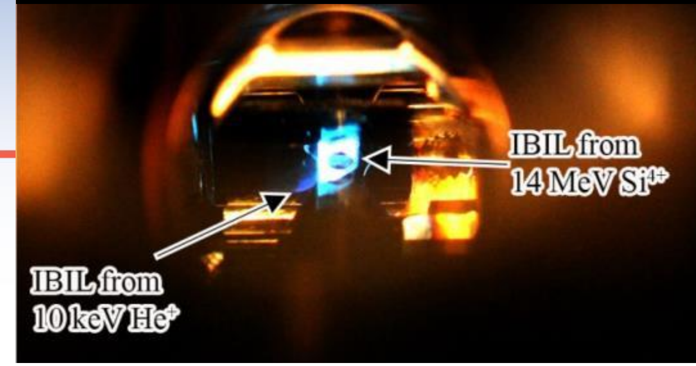

Direct real time observation of ion irradiation, ion implantation, or both with nanometer resolution

10 kV Colutron - 200 kV TEM - 6 MV Tandem

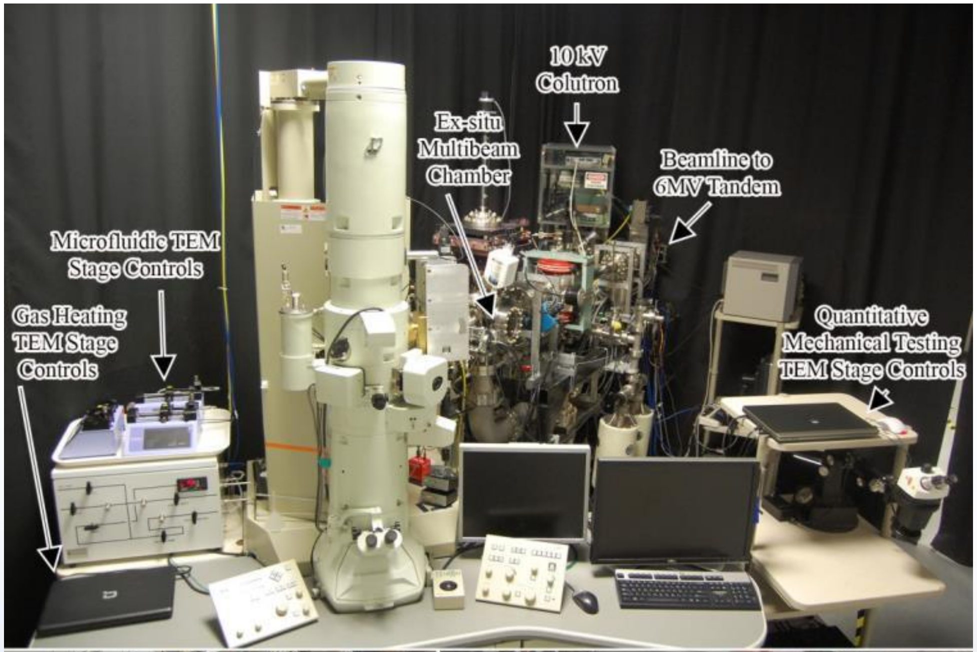

Ion species & energy introduced into the TEM

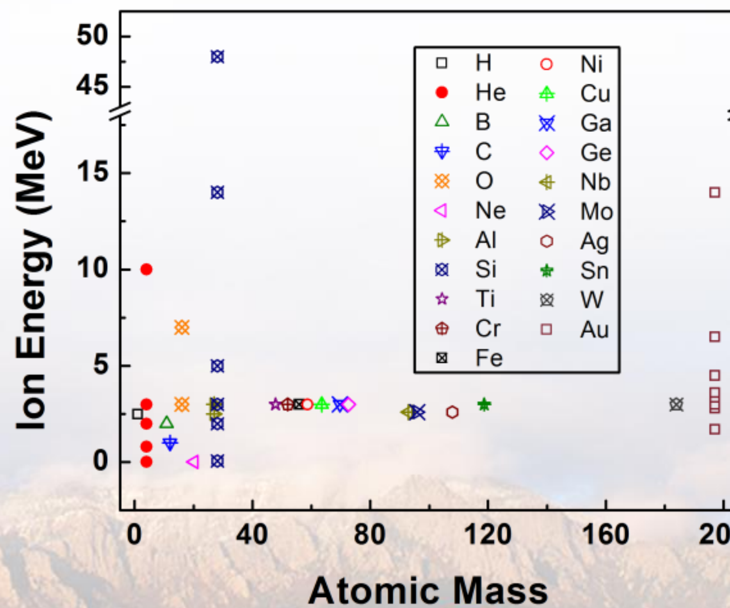

Benefits & Limitations of *in situ* TEM

Benefits

1. **Real-time nanoscale resolution observations of microstructural dynamics**

Limitations

1. **Predominantly limited to microstructural characterization**
   - Some work in thermal, optical, and mechanical properties
2. **Limited to electron transparent films**
   - Can often prefer surface mechanisms to bulk mechanisms
   - Local stresses state in the sample is difficult to predict
3. **Electron beam effects**
   - Radiolysis and Knock-on Damage
4. **Vacuum conditions**
   - 10^{-7} Torr limits gas and liquid experiments feasibility
5. **Local probing**
   - Portions of the world study is small

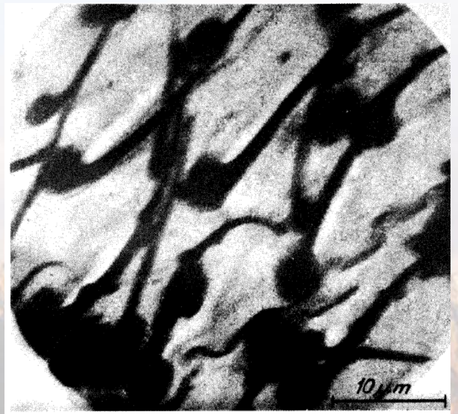

Fig. 6: Wing surface of the house fly.
(First internal photography, U = 60 kV, M$_u$ = 2200)
(Driest, E., and Müller, H.O.: Z. Wiss. Mikroskopie 52, 53-57 (1935)

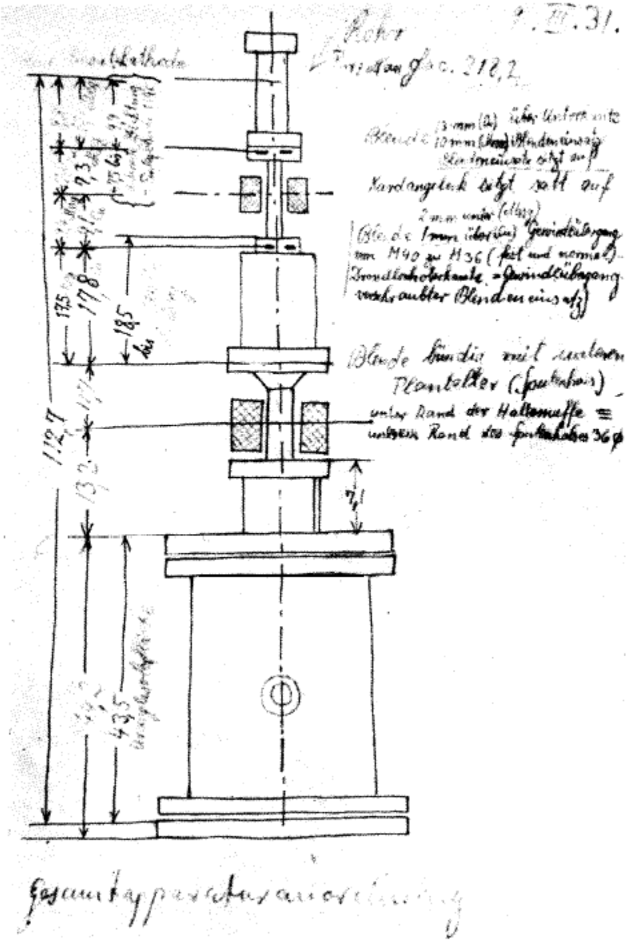

Fig. 2: Sketch by the author (9 March 1931) of the cathode ray tube for testing one-stage and two-stage electron-optical imaging by means of two magnetic electron lenses (electron microscope) [8].

E. Ruska Nobel lecture (1986)

$LiAlO_2$ Background

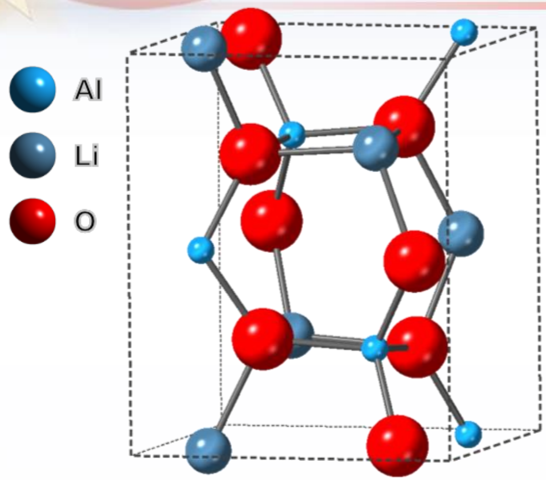

γ–$LiAlO_2$ is tetragonal (SG: P 41 21 2)

<u>Previous Work</u>

- Structural defects
  - Luo *et al* JNM 372 (2008) 53-58
- Volume swelling
  - Noda JNM 179-181 (1991) 37-41
- ^3H detrapping
  - Oyaidzu *et al* JNM 375 (2008) 1-7
- Gas diffusion and release
  - Raffray *et al* JNM 210 (1994) 143-160

- H isotopes are thought to trap in oxygen vacancies
  - ^2H release occurs at the same temperature as defect annealing in implanted $LiAlO_2$

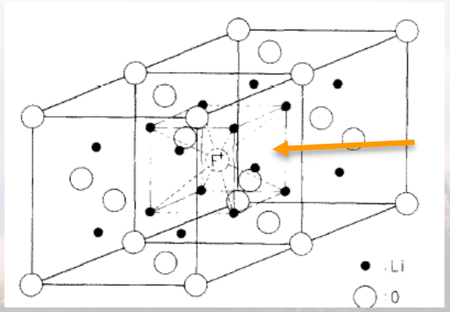

Noda JNM 179-181 (1991) 37-41

Can be determined with luminescence

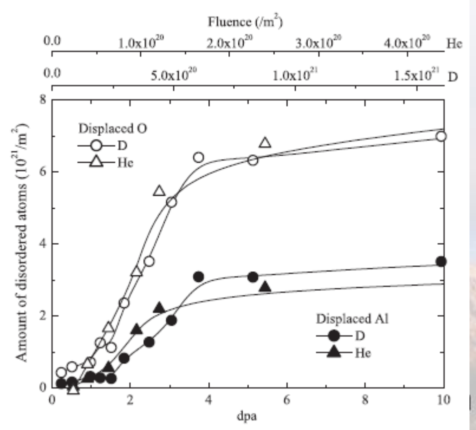

Katsui *et al.* NIMB 268 (2010 2735-2739

Previous work investigated $LiAlO_2$ powders and In-situ Ion Irradiation

- **Powders were drop-cast onto TEM grids**

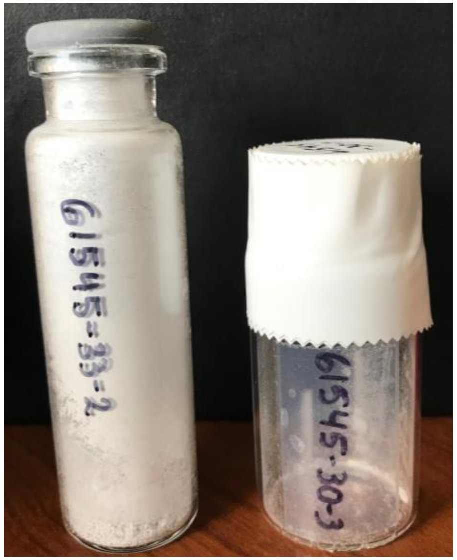

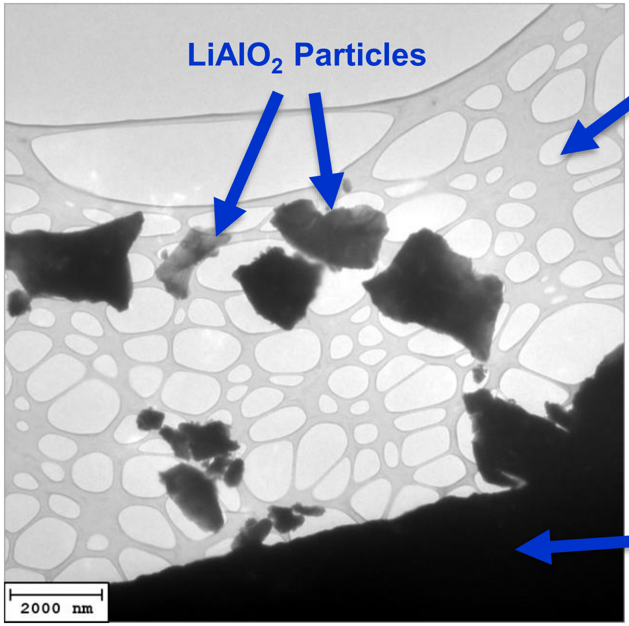

- **Samples were heated to 310°C using Hummingbird HT stage**
- **Four sets of irradiations:**
  - 200 keV electrons → simulates Gamma (γ) irradiation
  - 200 keV e⁻ +10 keV He → simulates γ and He accumulation from ^{6}Li transmutation and ^{3}H decay
  - 200 keV e⁻ + 10 keV He + 5 keV D → simulates γ , He, and ^{3}H interaction
  - 200 keV e⁻ + 10 keV He + 5 keV D + **1.7 MeV Au**→ simulates γ, gas build-up + cascades

Prior Work Showed Electrons Alone Induced Void Growth

- **Voids were observed to form under the electron beam in several particles**
- **Rate of void formation is not consistent between particles**
- **Possibly due to electron beam displacing Li and O atoms**

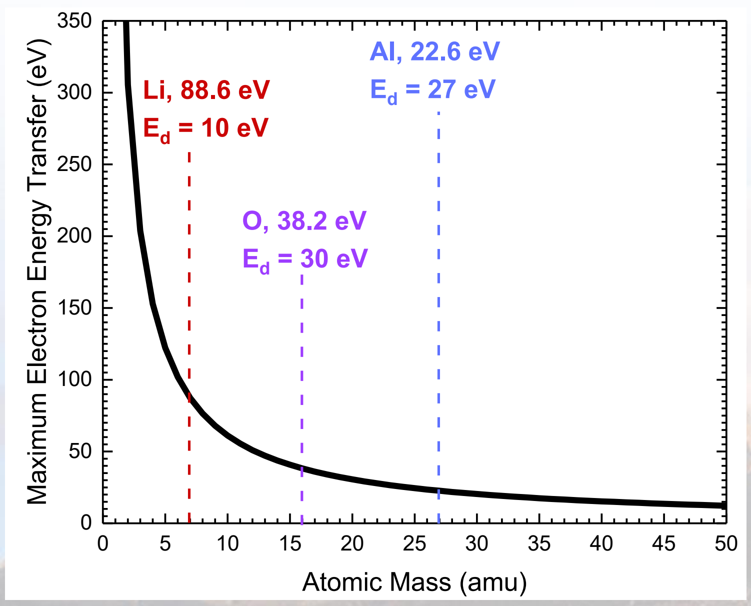

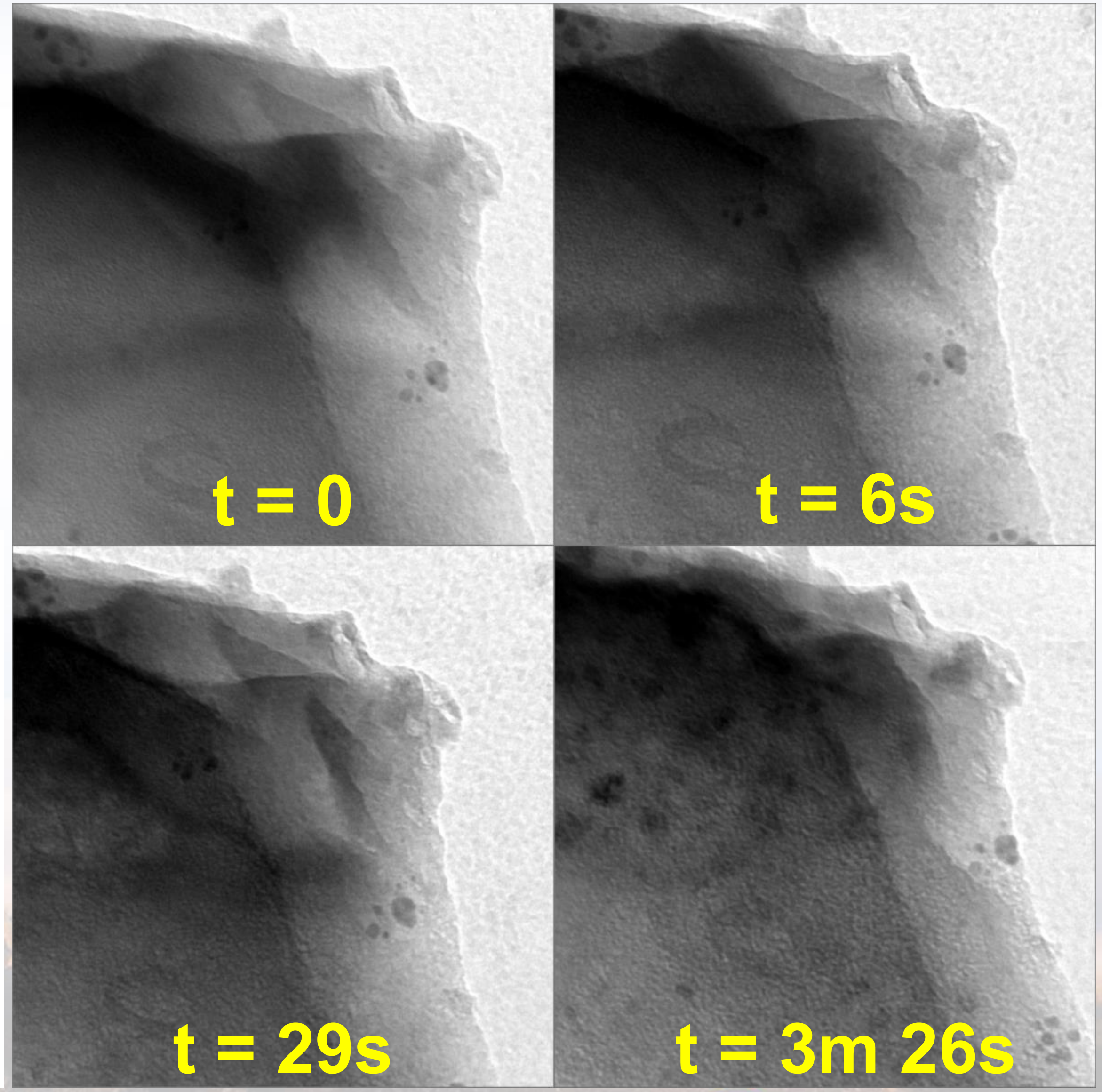

In-situ TEM He implantation at 310°C

- Each frame = 1 min of irradiation
- Because the voids are difficult to see in powders, I paused the video at a few points to show overfocus images
- Electron beam on for most of experiment
- Bubbles formed after ~13 min (1.5×10^{17} He/cm^2)

In-situ Video

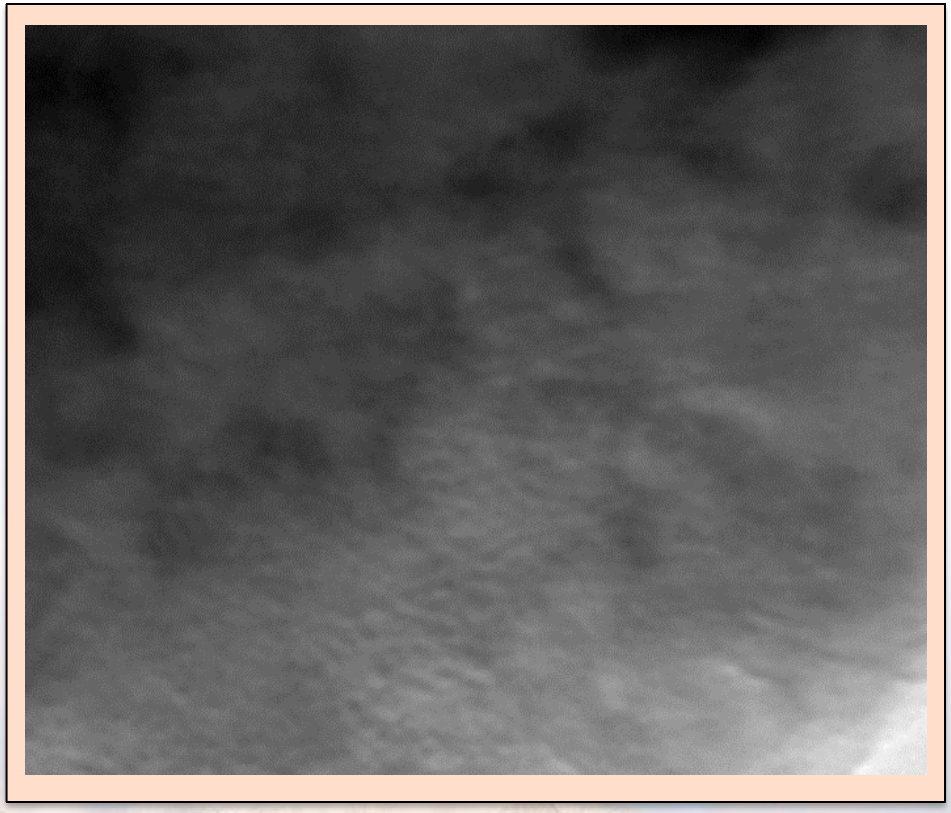

After Irradiation

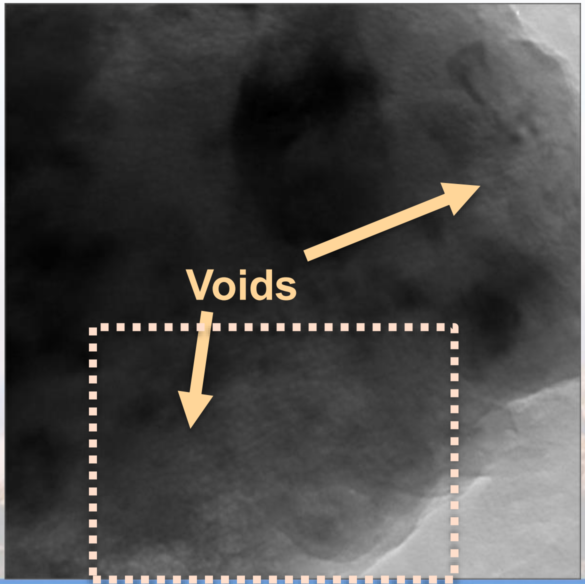

Sandia National Laboratories

In-situ TEM He & D irradiation at 310°C

- Each frame = 5 min of irradiation
- All underfocus images
- Electron beam was off except for imaging
- Bubbles formed after ~60 min (1.7×10^{17} He/cm^2, 3.4×10^{17} D/cm^2)

After Irradiation

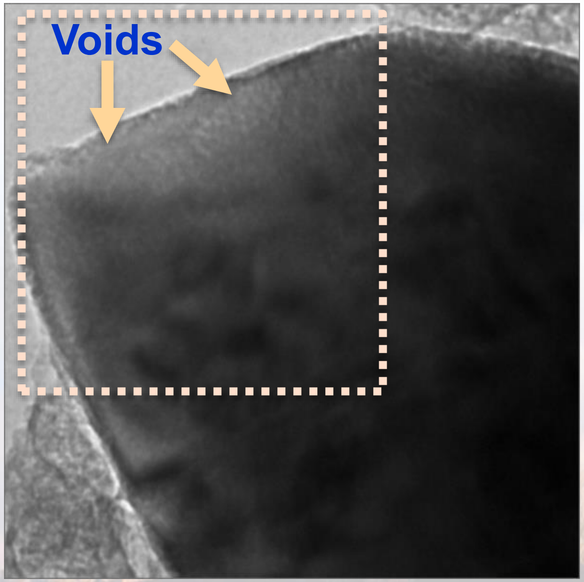

In-situ Video

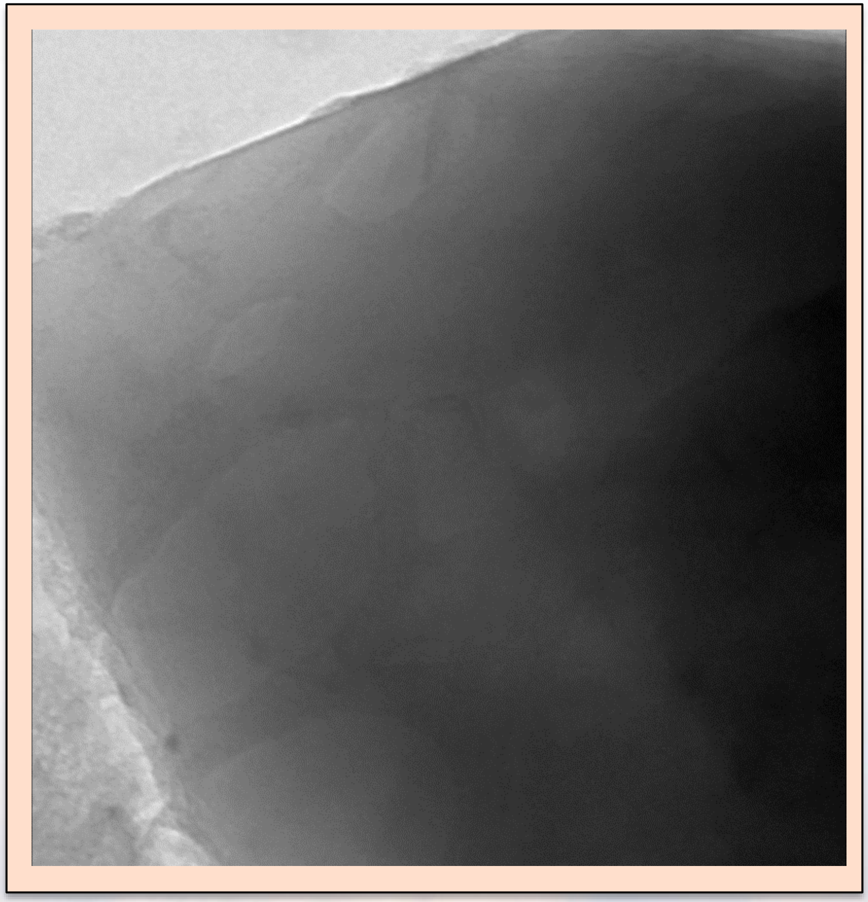

In-situ TEM He, D, & Au at 310°C

- Each frame = 5 min of irradiation
- Pre-existing voids could have an effect on this final microstructure
- Electron beam was on for most of the experiment

After Irradiation

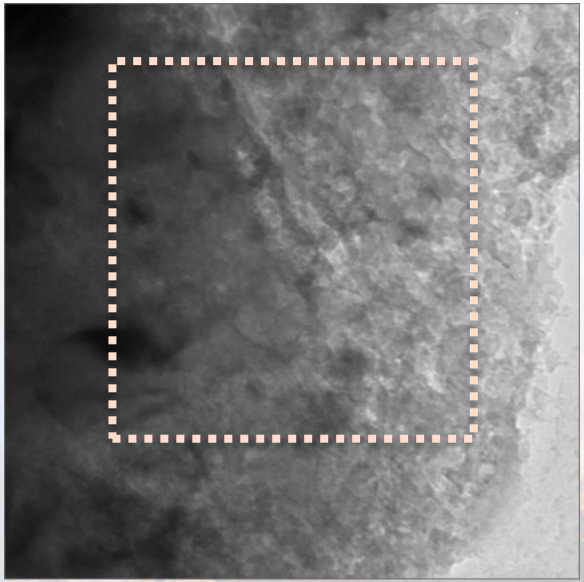

In-situ Video

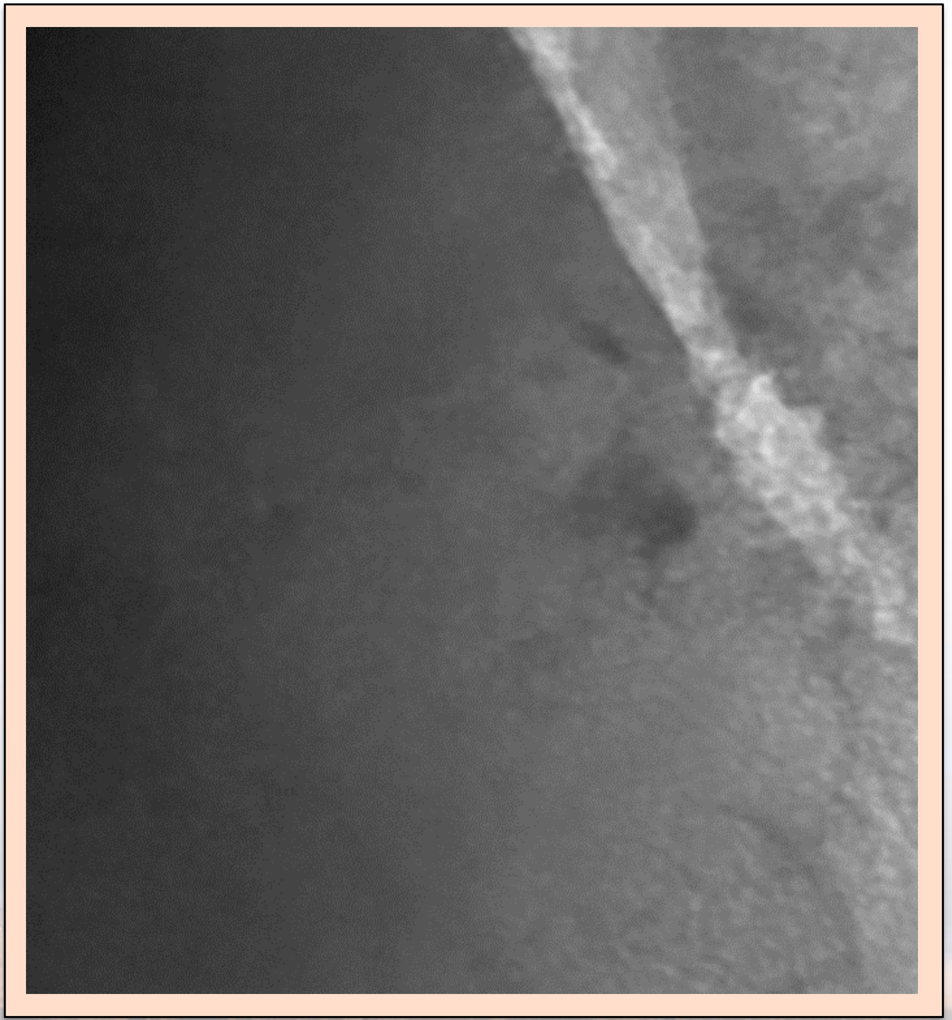

Prior work performed on powders: what affect does bulk material have?

- **Effect of crystal orientation and grain boundaries**
- **TEM lamella of single-crystal and poly-crystalline lithium aluminate prepared**
- **Lamella irradiated ex-situ with He and H**
  - Room temperature
  - 10 keV H/He
  - Single Crystal: 10 keV He to a-b) $1x10^{17}$ and c-d) $5x10^{18}$
    - Post-implantation annealing to 200 ° C and 450 ° C
  - Polycrystalline: 10 keV H to a-d) and 10 keV He to a-b) $1x10^{17}$ and c-d) $5x10^{18}$
    - Post-implantation annealing to 200 ° C and 450 ° C

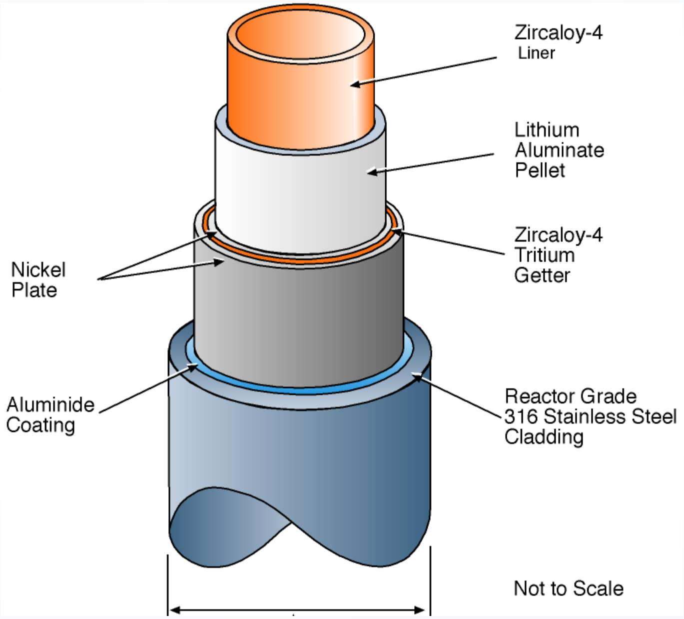

He implantation dose plays a significant role in He bubble formation

$1x10^{17}$ He

$5x10^{18}$ He

As-implanted

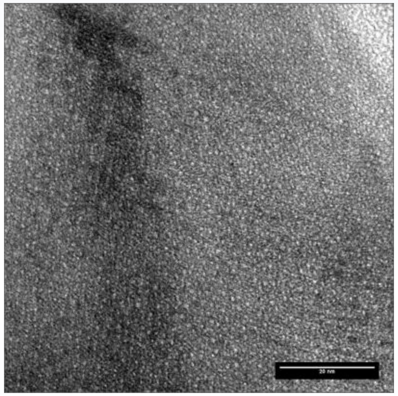

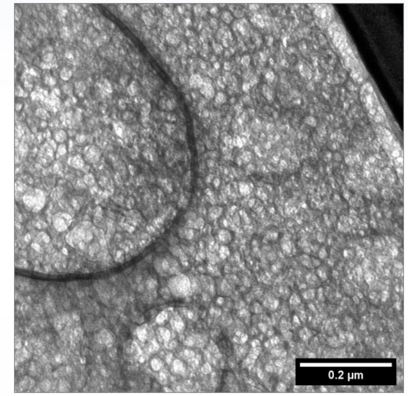

200 C

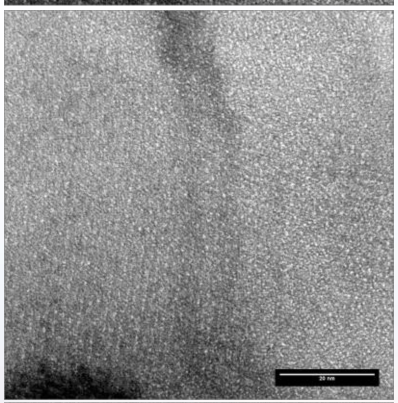

Low dose: He bubbles grow significantly

High Dose: Less obvious bubble growth

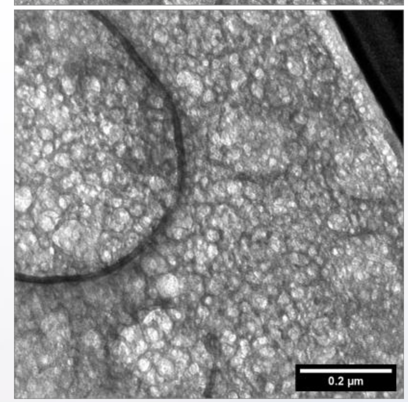

450 C

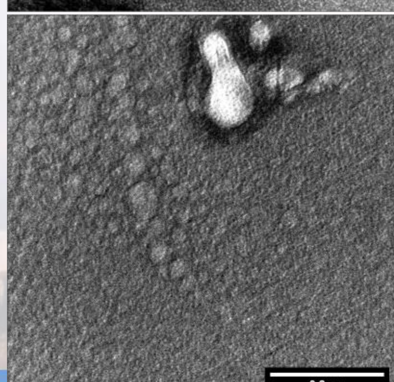

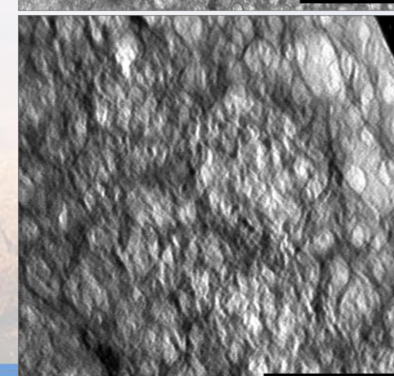

Annealing of single crystal lamella results in bubble growth at low fluence

	Pre-Anneal (nm)	Post Anneal
$1x10^{17}$ - 200 C	2.86 nm	1.21 nm
$1x10^{17}$ - 450 C	2.53 nm	4.98 nm
$5x10^{18}$ - 200 C	14.0 nm	14.8 nm
$5x10^{18}$- 450 C	3.61 nm	4.99 nm

But: lithium aluminate in TPBAR applications is not single crystal!

Polycrystalline annealing of lithium aluminate

$1x10^{17}$ H + $1x10^{17}$ He | **$1x10^{18}$ H + $5x10^{18}$ He**

As-implanted

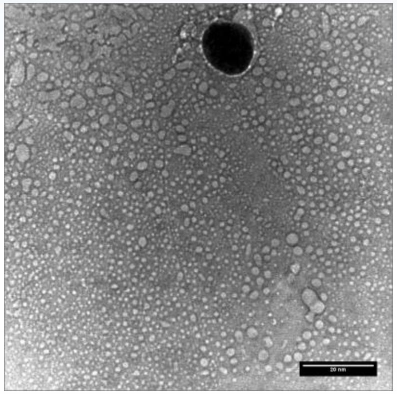

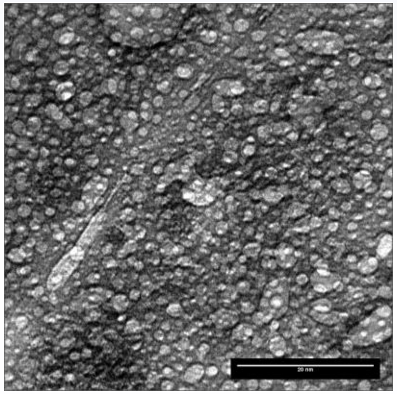

200 C

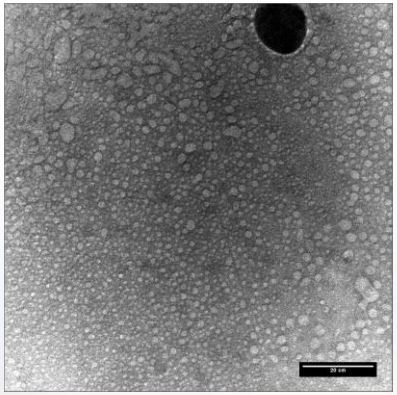

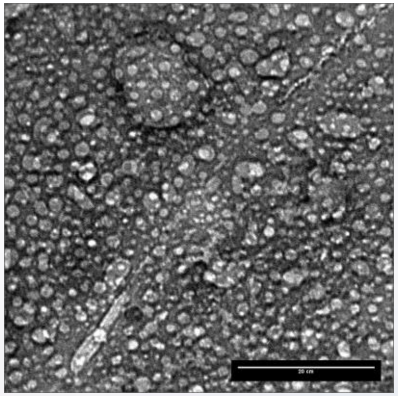

Little evidence of bubble growth

Grain boundaries arresting bubble growth?

Also, have the added consideration of H irradiation

450 C

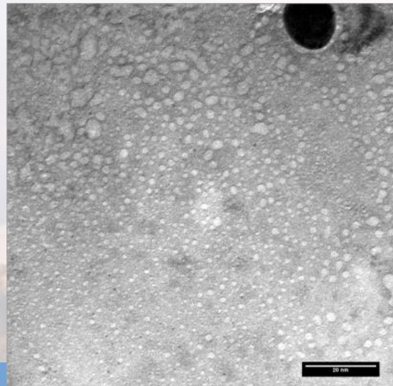

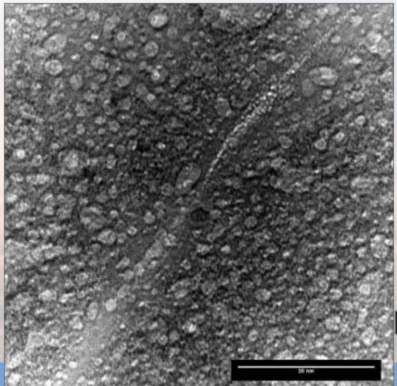

Laboratories

Polycrystalline samples show larger He bubbles and accumulation at grain boundaries

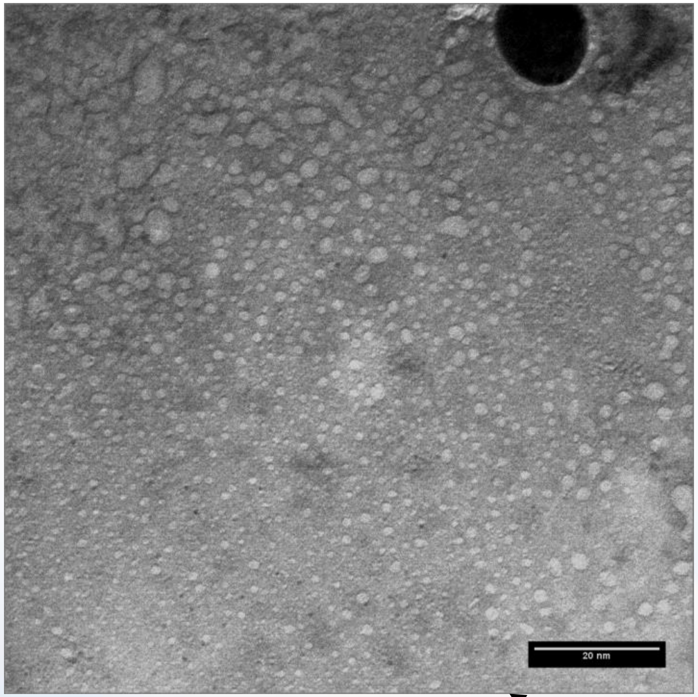

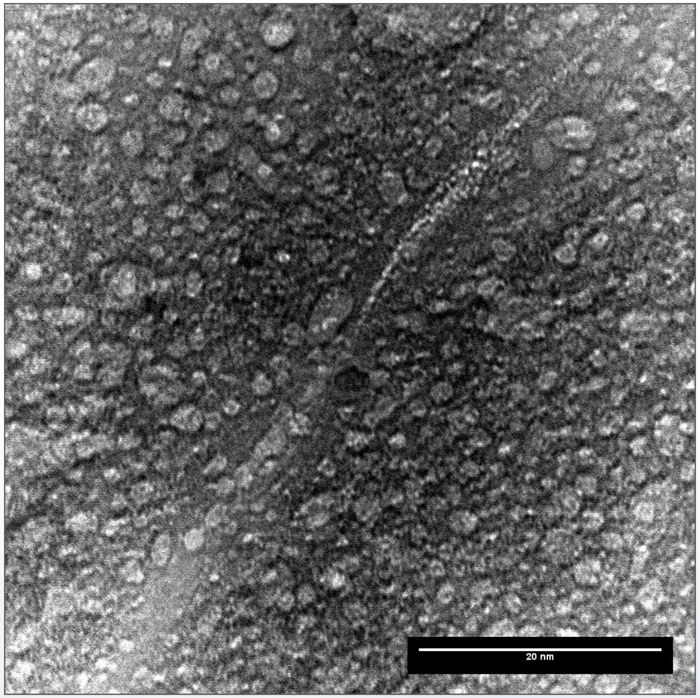

But: No evident growth via Migration and Coalescence or Oswald Ripening

Sandia National Laboratories

Summary

$LiAlO_2$

Single Crystal He → High Dose → Polycrystalline He+H

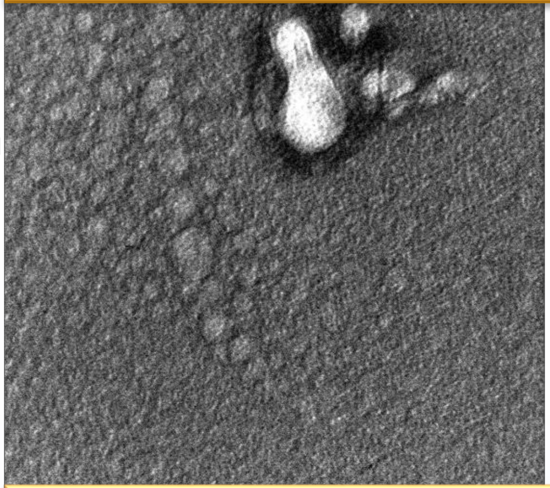

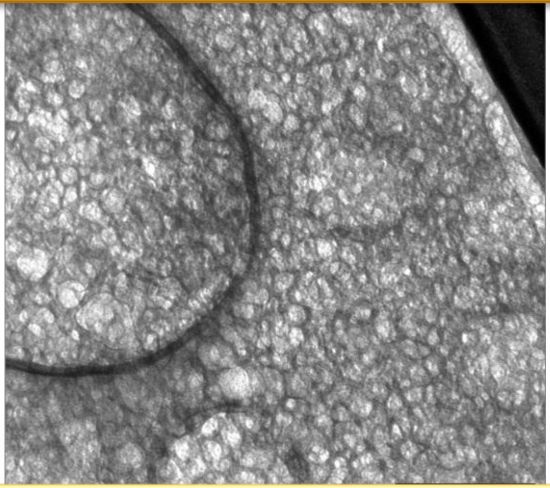

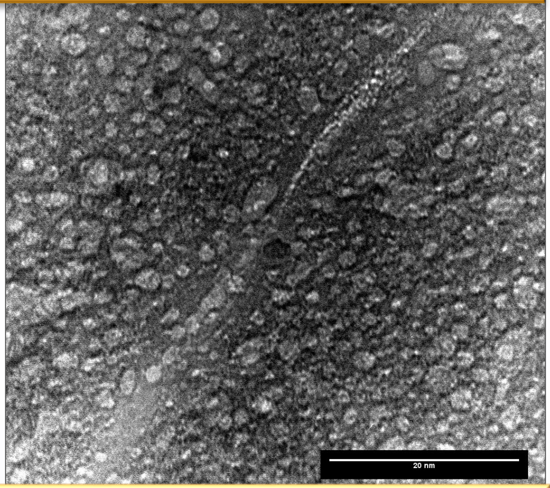

$LiAlO_2$ Powder

He accumulation → ^3H + He → Damage + He + ^3H

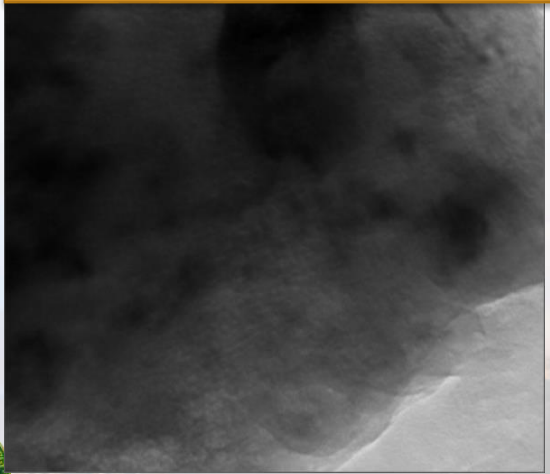

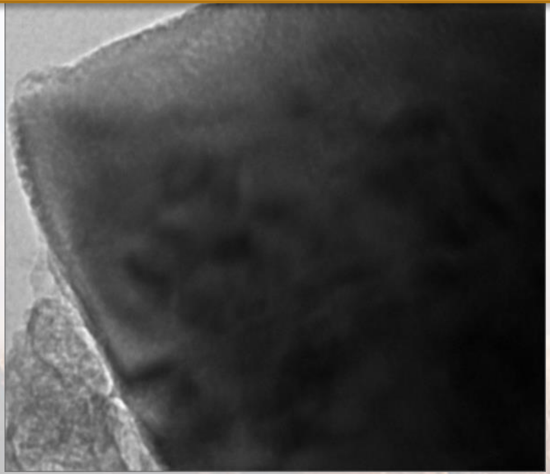

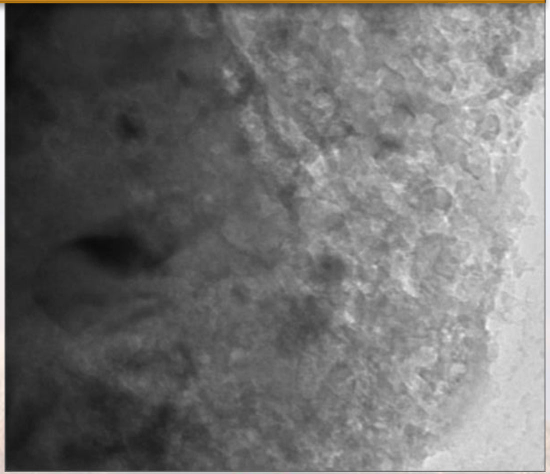

Precession Electron Diffraction Post He Implantation and Annealing Reveals Hidden Grain Structure

Cavities in helium implanted, self-ion irradiated,

nc nickel film annealed to 400 ˚C

Cavities span multiple grains at identified grain boundaries

Same to be done with lithium aluminate

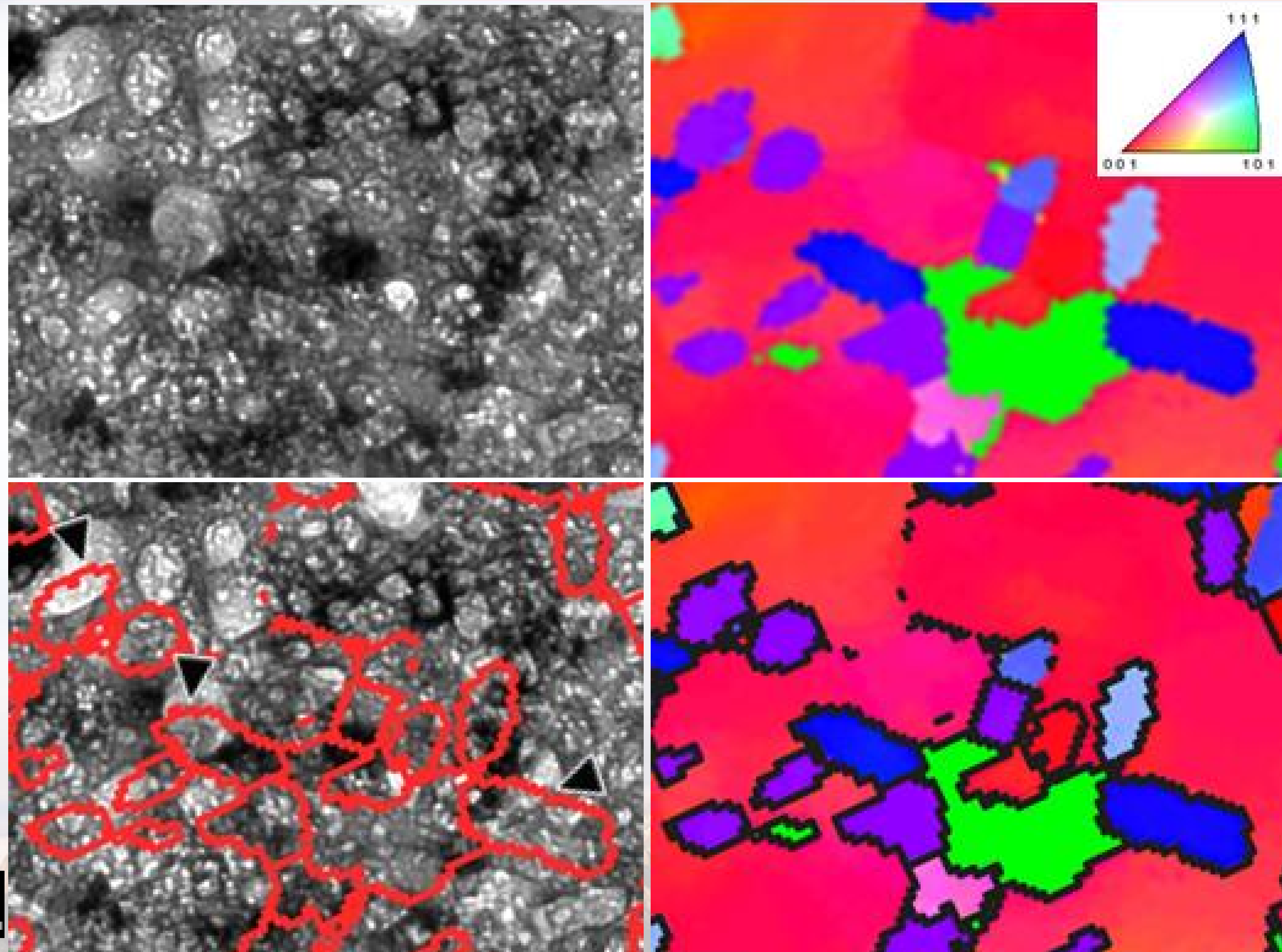

100 nm

Grain structure of lithium aluminate impacts the He accumulation

- Bulk lithium aluminate used as neutron absorber in TPBAR applications
- Prior in-situ TEM work only performed on powders – not representative of bulk
- In-situ and ex-situ H/He irradiation of bulk single crystal and polycrystalline lithium aluminate performed
- Grain boundaries accumulate He, grain orientation affects He bubble size, shape, and density

Summary

- **Sandia's I^{3}TEM capabilities:**
  - ***In situ*** **high energy ion irradiation from H to Au**
  - ***In situ*** **gas implantation**
  - **Heating up to 1,000 ˚C**
  - **Quantitative and bulk straining**
  - **Two-port microfluidic cell**
  - **Gas flow/heating stage**
  - **Electron tomography**
  - **Precession Electron Diffraction**
  - **Laser heating with 20W 1064nm laser**
  - **To be installed: in-situ Raman and PL**

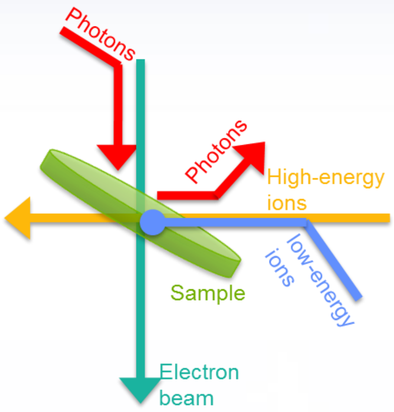

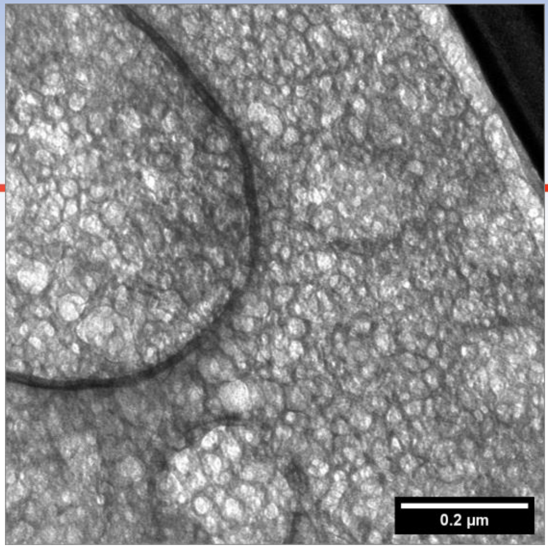

Sandia's I^{3}TEM provides a wealth of interesting initial observations and harsh environments with in-situ irradiation and annealing

- **Currently applying the current I^{3}TEM capabilities to various material systems in combined and harsh environmental conditions**

Collaborators:

- **IBL: D.C. Bufford, D. Buller, C. Chisholm, B.G. Clark, J. Villone, B.L. Doyle, S. H. Pratt, M. Steckbeck & M.T. Marshall**
- **Sandia: B. Boyce, T.J. Boyle, P.J. Cappillino, J.A. Scott, B.W. Jacobs, M.A. Hekmaty, D.B. Robinson, J.A. Sharon, W.M. Mook, F. Abdeljawad, & S.M. Foiles**
- **External: A. Minor, L.R. Parent, I. Arslan, H. Bei, E.P. George, P. Hosemann, D. Gross, J. Kacher, & I.M. Robertson**

This work was partially supported by the US Department of Energy, Office of Basic Energy Sciences.
Sandia National Laboratories is a multi-mission laboratory managed and operated by National Technology & Engineering Solutions of Sandia, LLC., a wholly owned subsidiary of Honeywell International, Inc., for the U.S. Department of Energy's National Nuclear Security Administration under contract DE-NA0003525.

NSUF Nuclear Science User Facilities

Sandia National Laboratories

Back-up Slides

In-situ TEM He implantation at 310°C

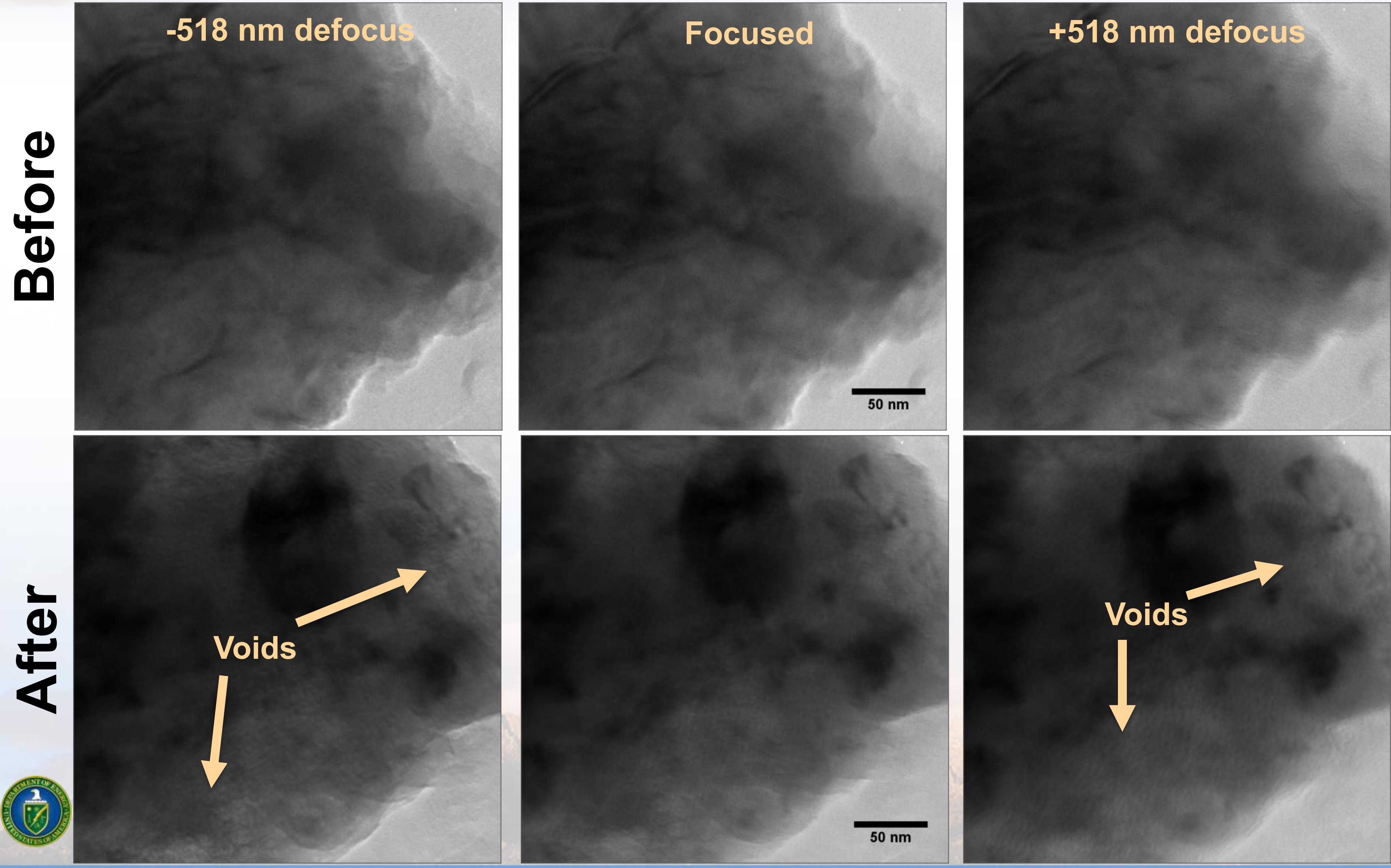

In-situ TEM He & D irradiation at 310°C

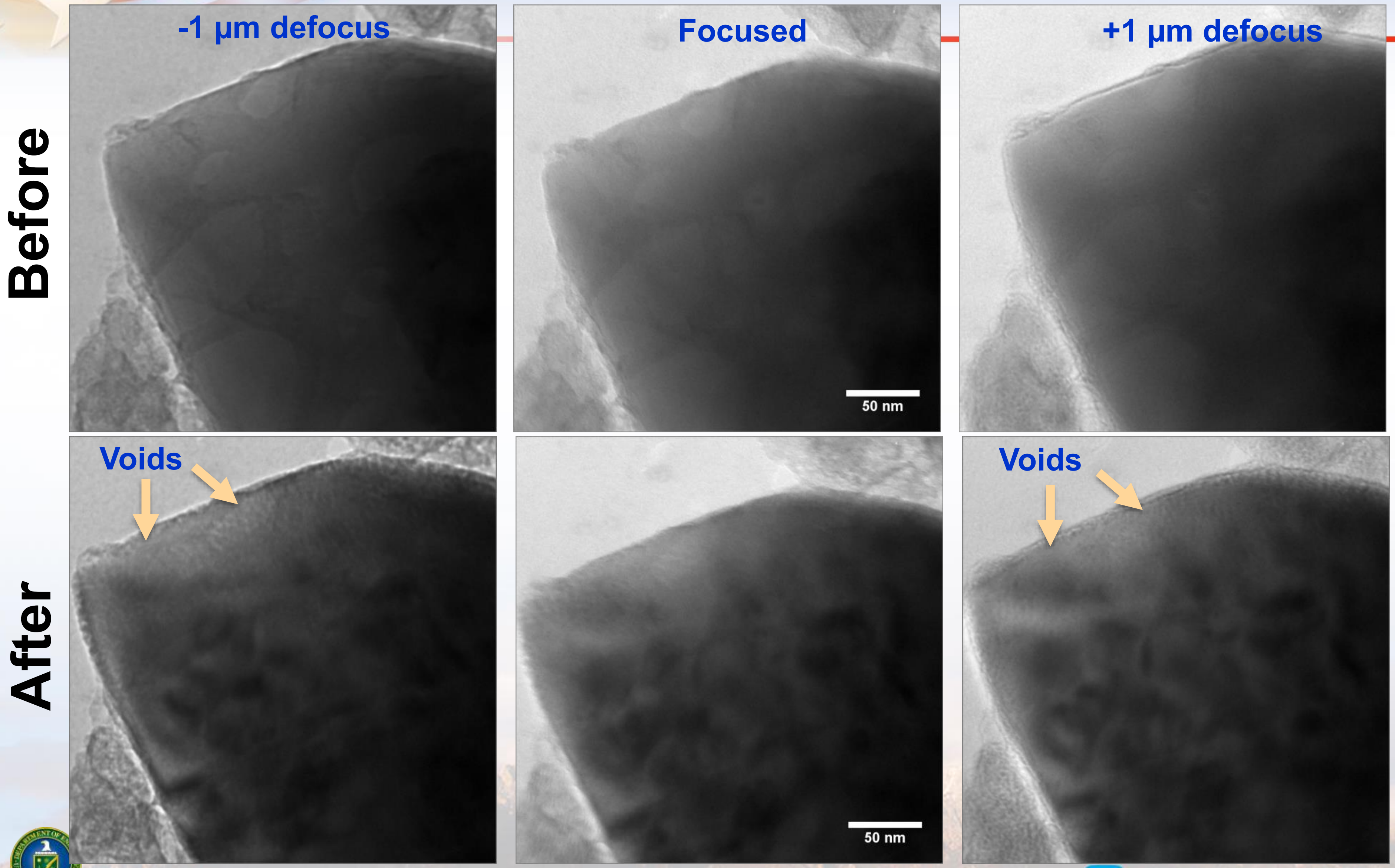

Sandia National Laboratories

In-situ TEM He, D, & Au at 310°C

Before

After

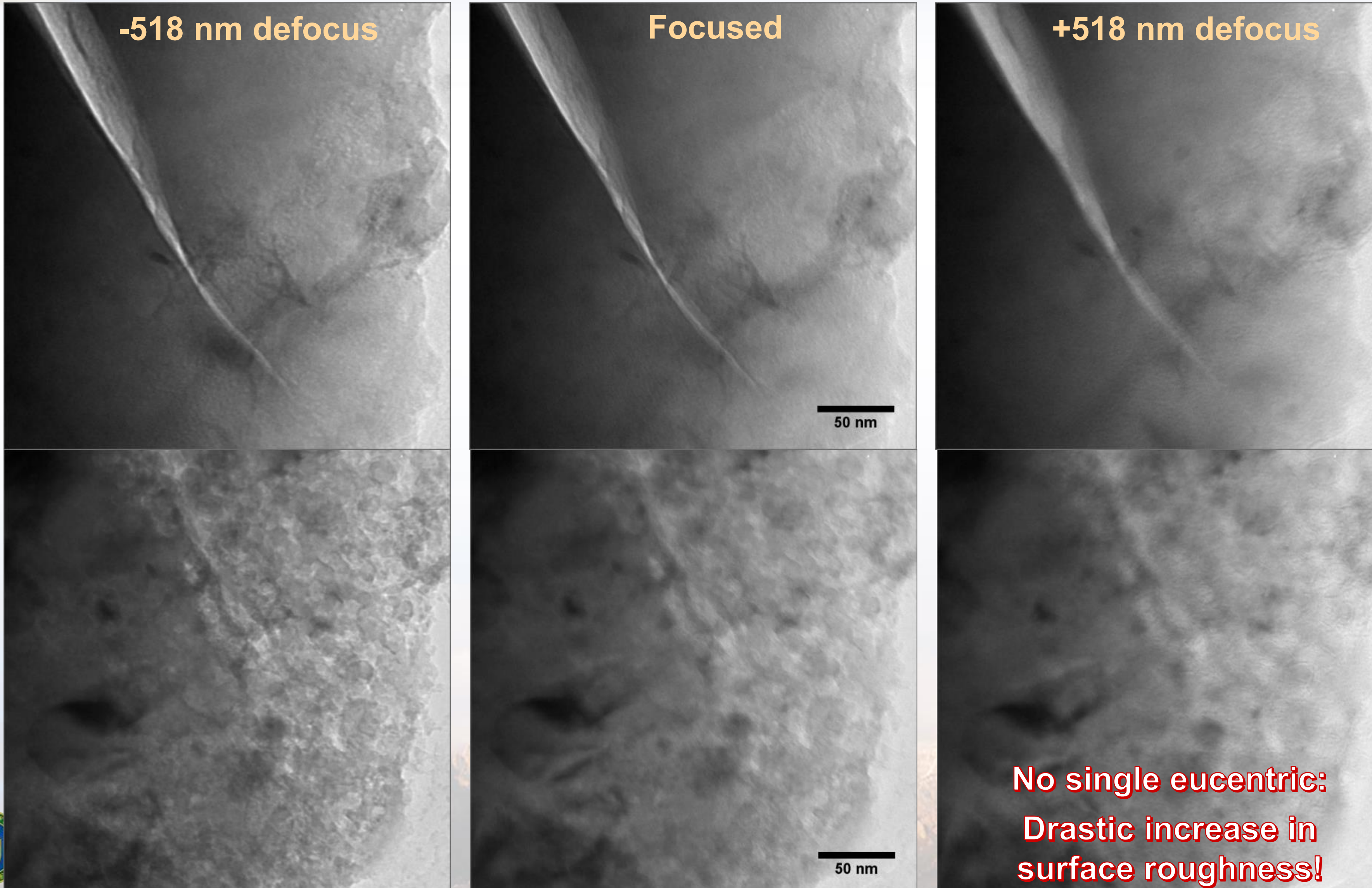

Tritium Producing Burnable Absorber Rod

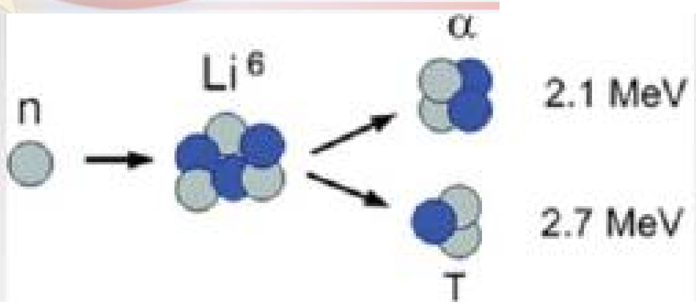

- Displacement Damage
- Helium Implantation
- Tritium Implantation
- Elevated Temperatures

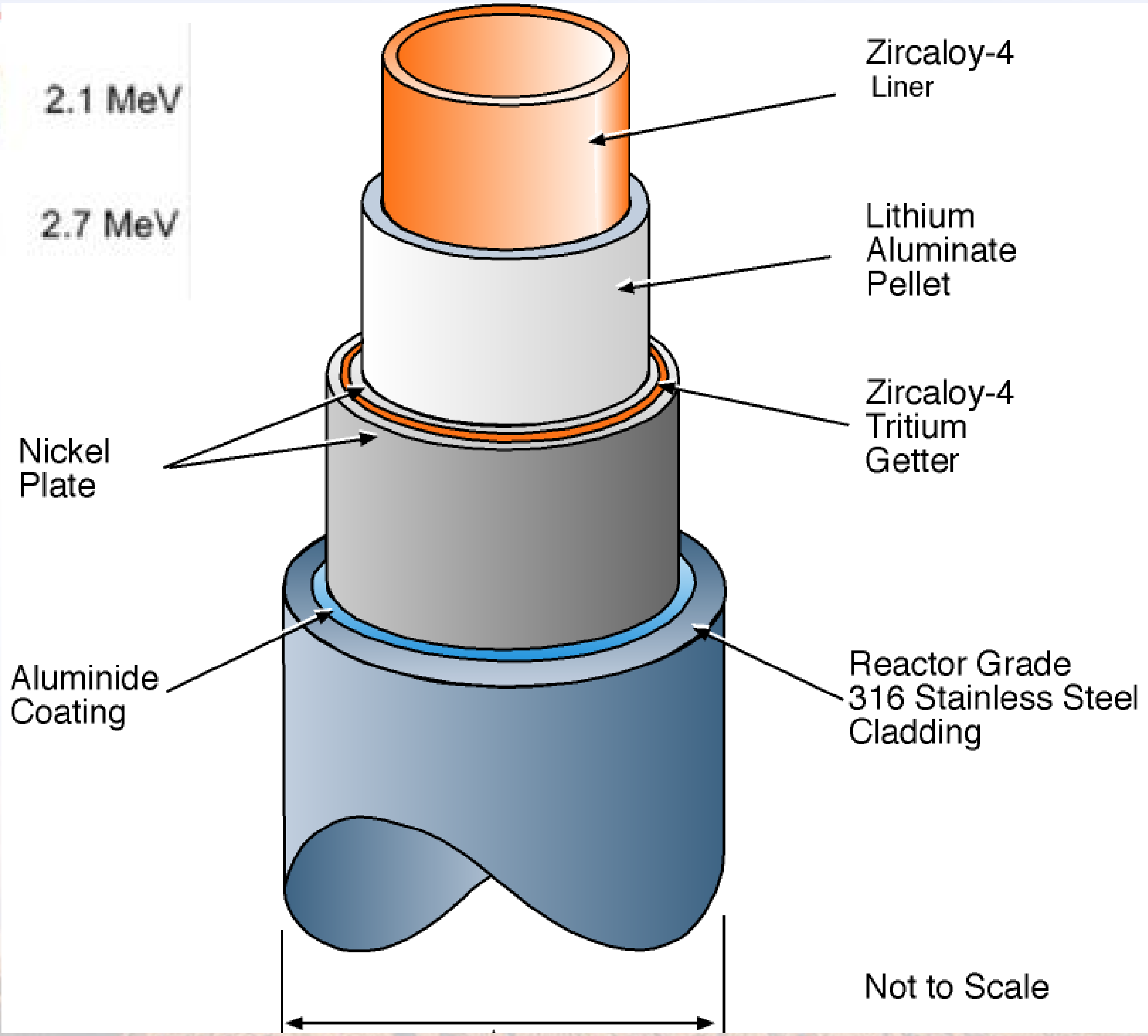

Zircaloy Background

<u>What is Zircaloy?</u>

- Zircaloy-2: predominantly used as fuel cladding for BWRs
  - α-Zr, 1.5% Sn, 0.15% Fe, 0.1% Cr, 0.05% Ni
- Zircaloy-4: Removed the Ni and increased Fe content for less H uptake in certain reactor conditions
  - α-Zr, 1.5% Sn, 0.2% Fe, 0.1% Cr
- Zr-Nb alloys (e.g. Zirlo) are also common
- α-Zr has a hexagonal close-packed (HCP) crystal structure up to 810ºC

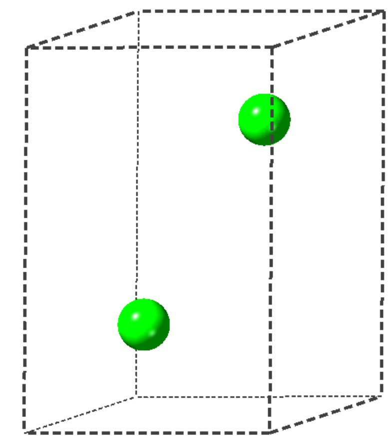

Crystal Structure of α-Zr (HCP)

<u>Gas and defect behavior in Zr/Zr alloys</u>

- ^{3}H, H, and He diffusion and release
- Bubble formation
- Irradiation induced metallic precipitate formation

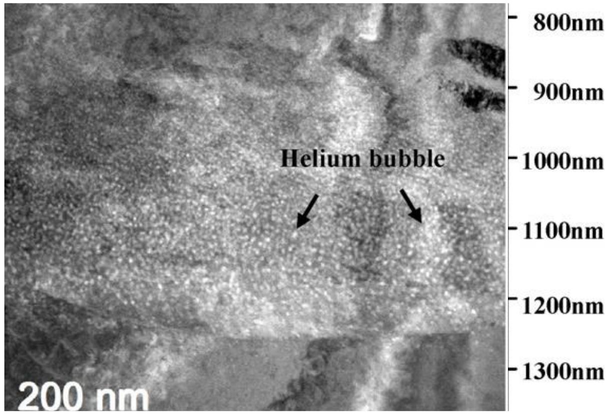

He bubbles in Zr-Nb alloy
Shen et al Mat Char 107 (2015) 309-316

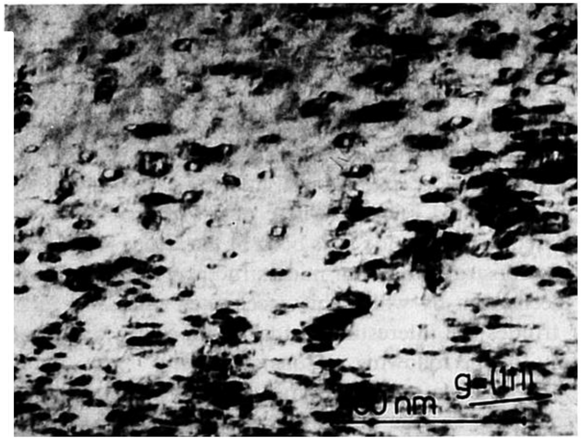

TEM of Zr tritide after 325d
Schober et al JNM 141-143 (1986) 453-457

Zr alloy in-situ ion irradiation parameters

- **Samples were prepared by electropolishing zirconium alloy samples (mostly ZIRLO)**
- **Several sets of irradiations done at 310°C, including:**
  - 10 keV He → simulates He accumulation from ^{6}Li transmutation and ^{3}H decay
  - 10 keV He + 5 keV D + **3 MeV Zr**→ simulates gas build-up + displacement cascades
- **SRIM, a Monte Carlo based program for simulating the number of displacements produced by an ion, was used to predict damage dose and concentration profiles.**
- **These preliminary experiments were run overnight and the exact gas concentrations/damage doses are not all known**

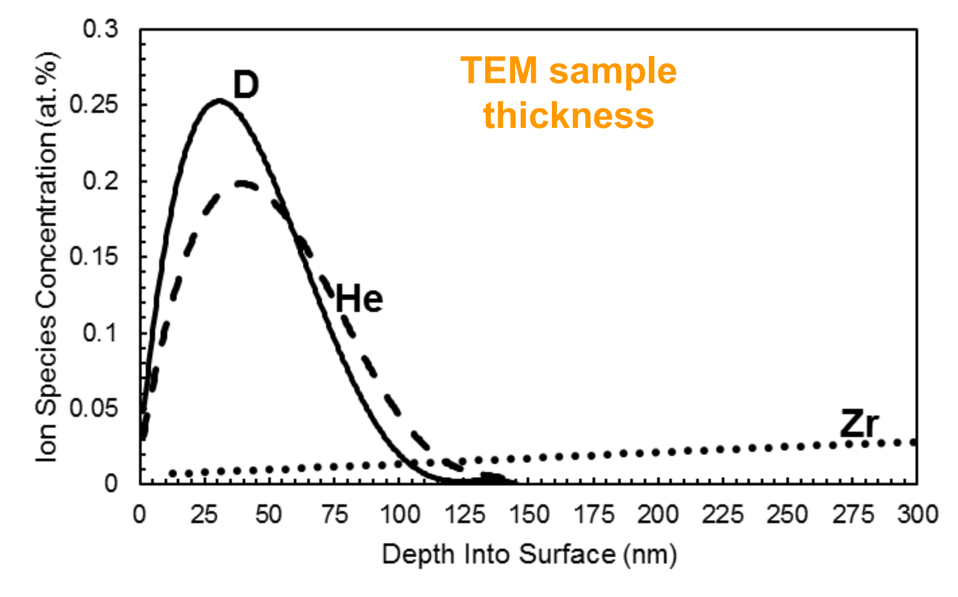

He and D profiles are implanted within the TEM sample, while most Zr passes through the sample, leaving only cascade damage.

10 keV He^{+} Implantation at 310°C

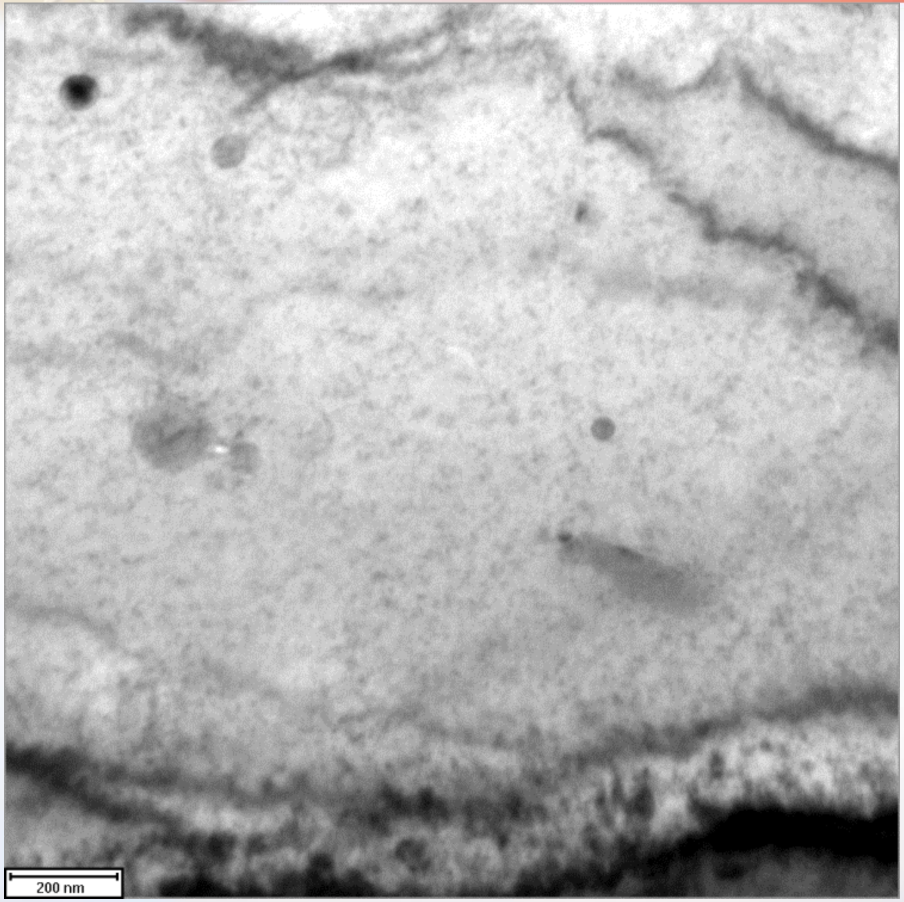

After Implantation.
Damage, No Cavities.

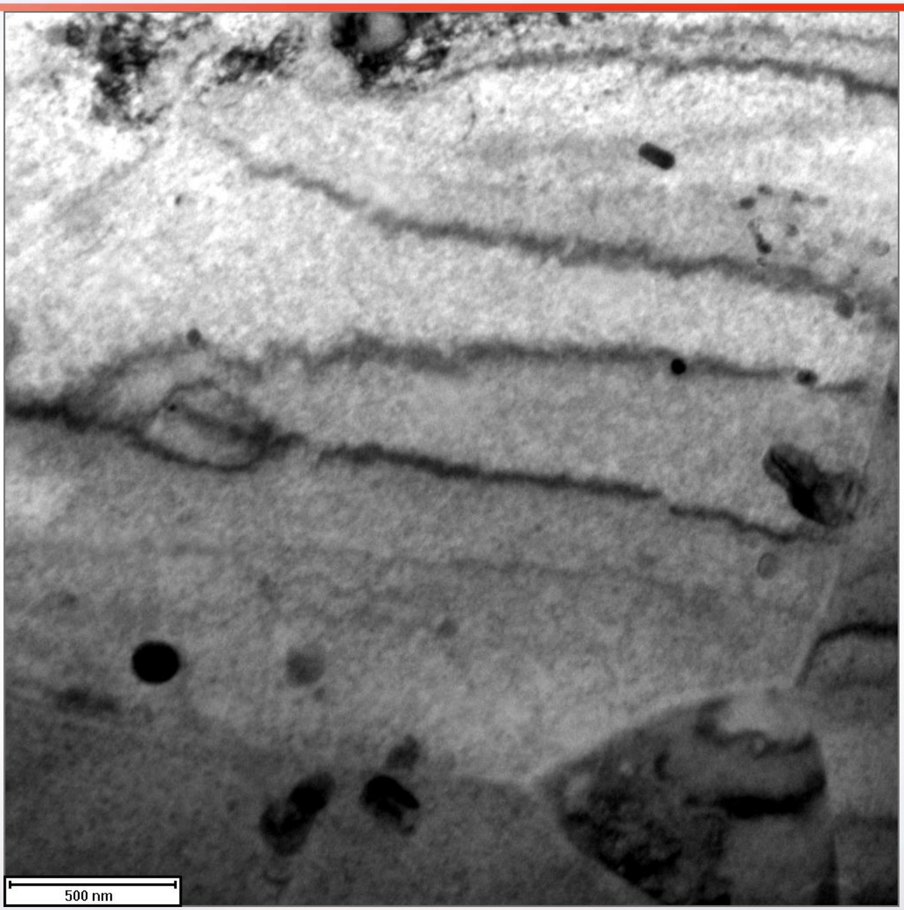

Still no cavities after subsequent irradiation with 3 MeV Zr.

Concurrent D & He Implantation & Zr Irradiation

After triple beam irradiation

- Very dense, complex defect structure
- No visible cavities
- Fuzzy defects difficult to characterize

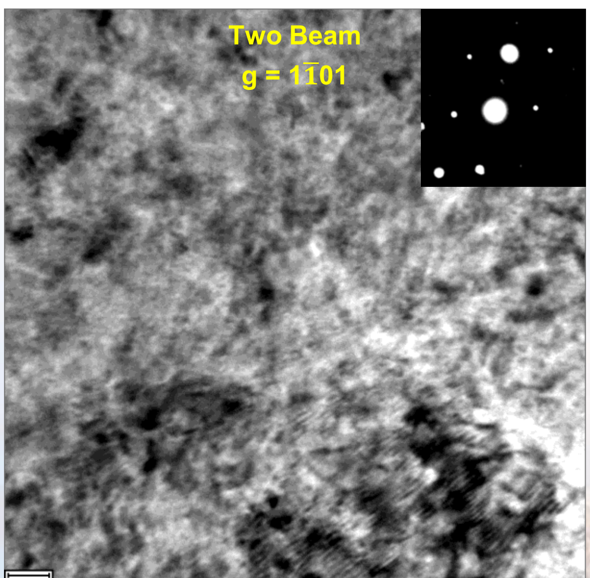

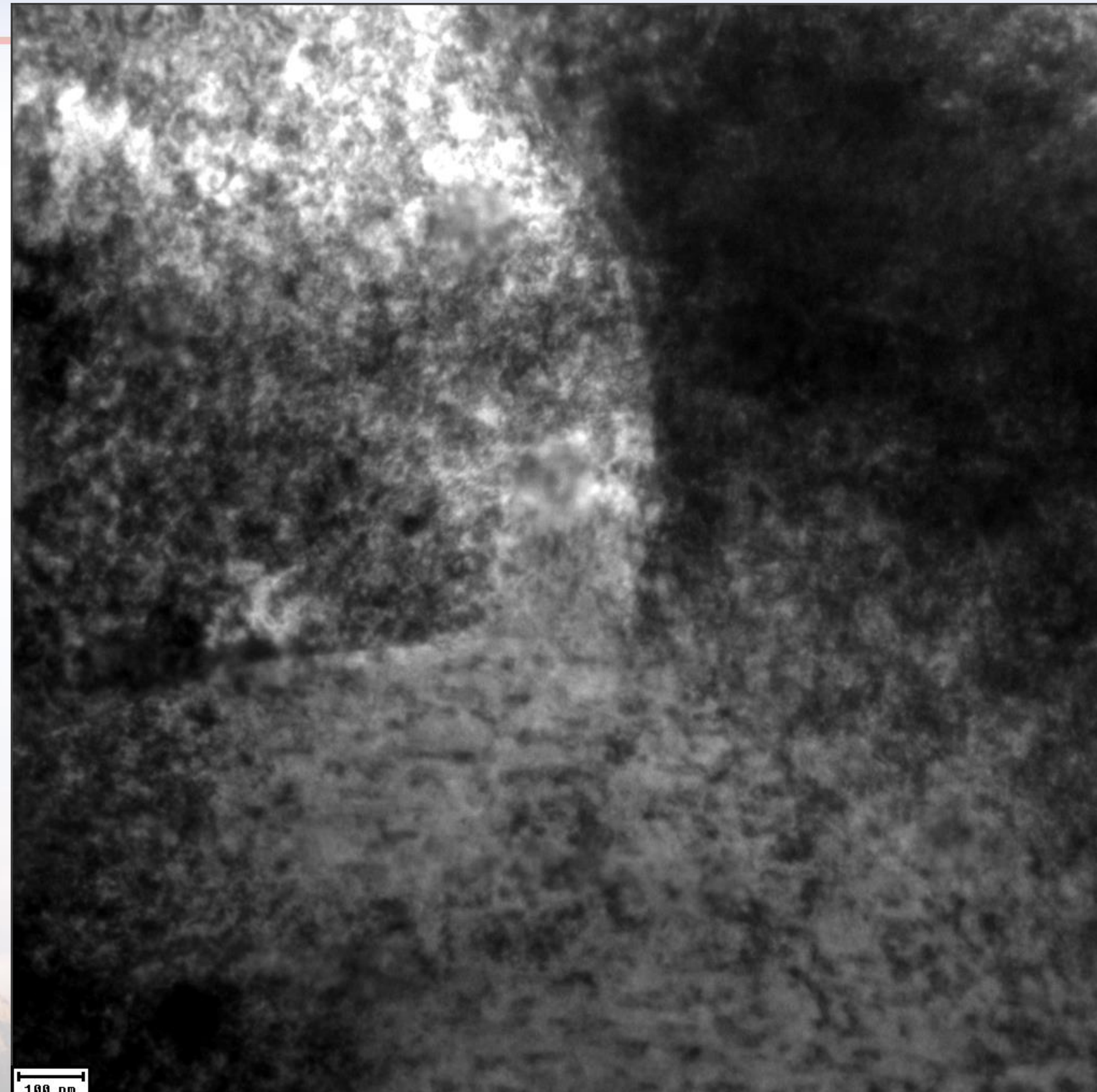

Cavities were observed in He implanted Zr alloy samples 30 days after irradiation

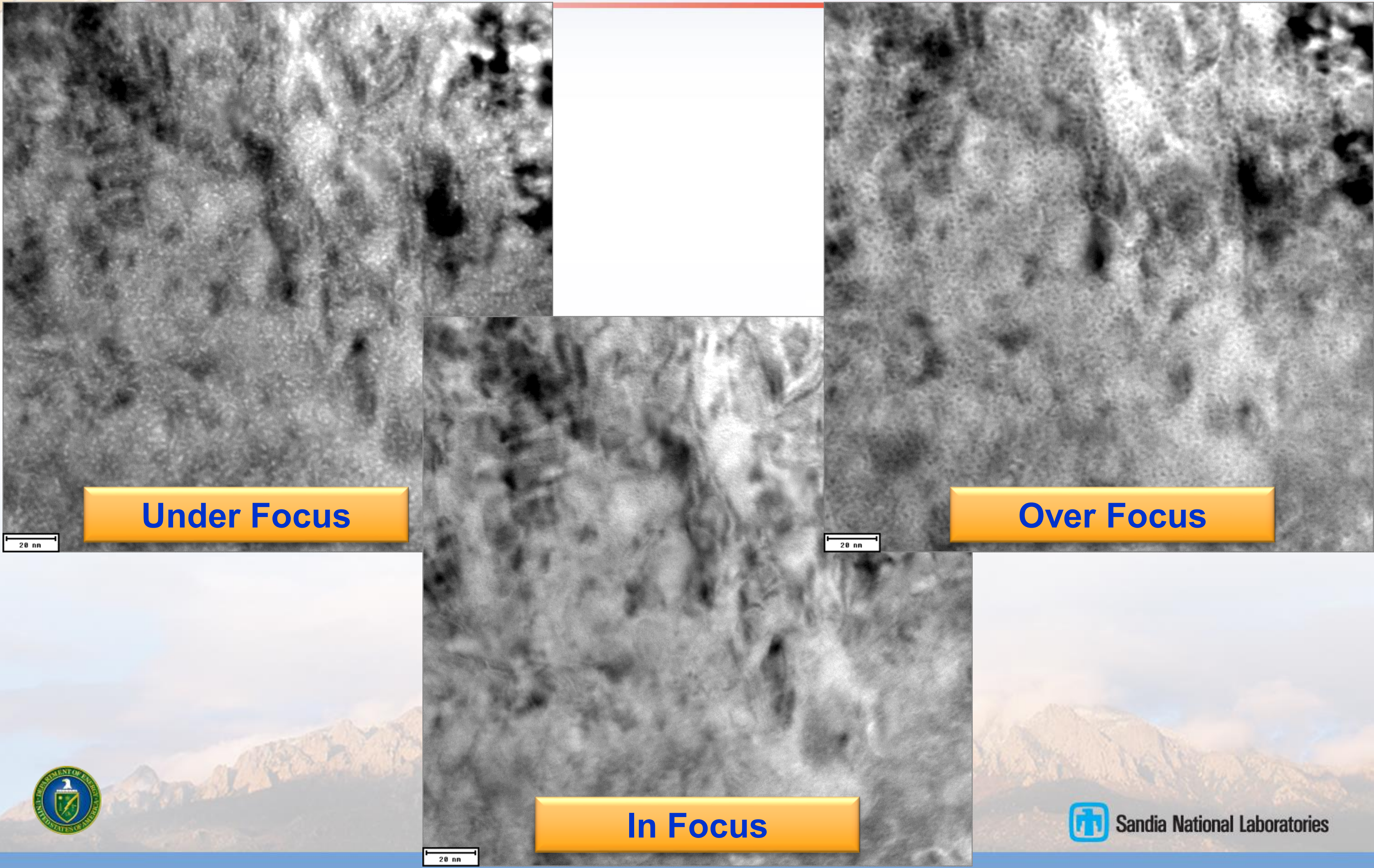

In situ TEM Hydrogen Exposure

Contributors: B.G. Clark, P.J. Cappillino, B.W. Jacobs, M.A. Hekmaty, D.B. Robinson, L.R. Parent, I. Arslan. & Protochips, Inc.

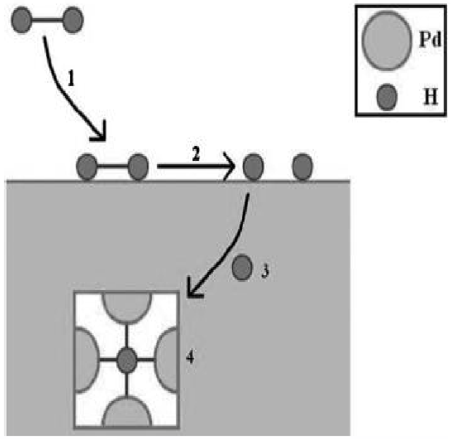

R. Delmelle, J., Phys. Chem. Chem. Phys. (2011) p.11412

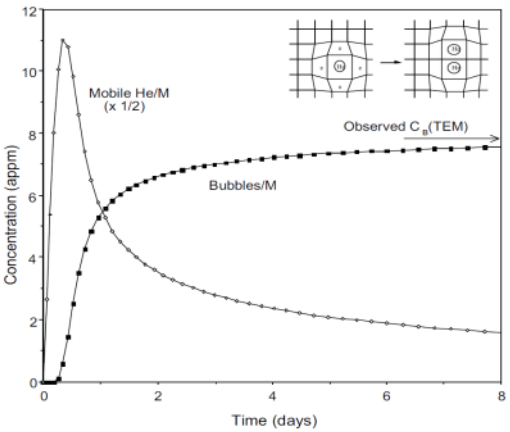

Cowgill, D., Fusion Sci. & Tech., 28 (2005) p. 539
Trinkaus, H. *et al*., JNM (2003) p. 229
Thiebaut, S. *et al*. JNM (2000) p. 217

Vapor-Phase Heating TEM Stage

- Compatible with a range of gases
- *In situ* resistive heating
- Continuous observation of the reaction channel
- Chamber dimensions are controllable
- Compatible with MS and other analytical tools

Harmful effects may be mitigated in nanoporous Pd

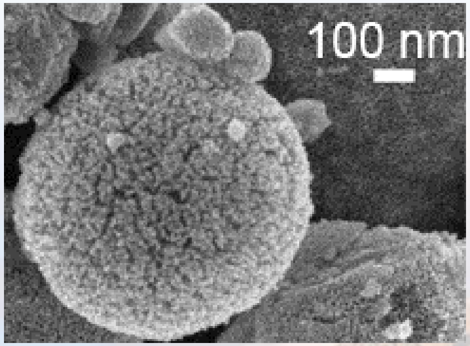

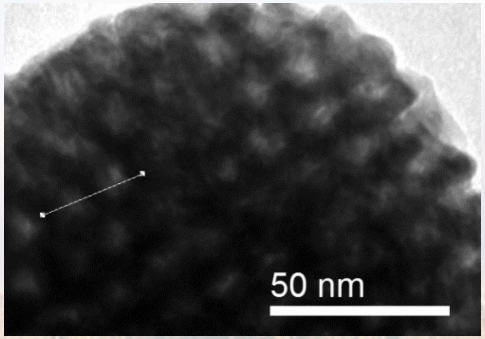

- 1 atm H_2 after several pulses to specified temp.

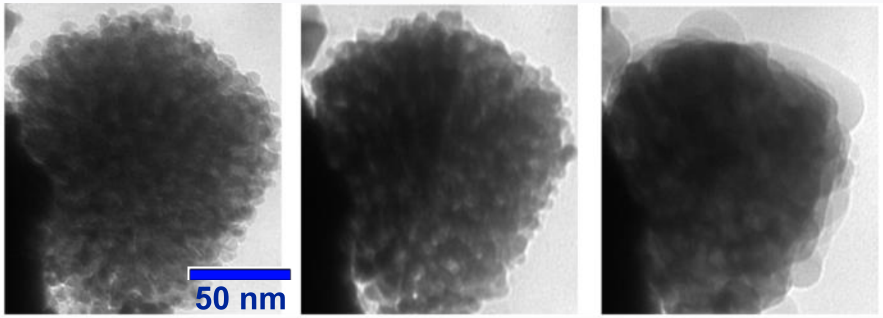

125° C | 200° C | 300° C

New *in situ* atmospheric heating experiments provide great insight into nanoporous Pd stability

Simulations of Damage and Gas Accumulation in TPBAR Materials with In-situ Triple Ion Beam Irradiation TEM

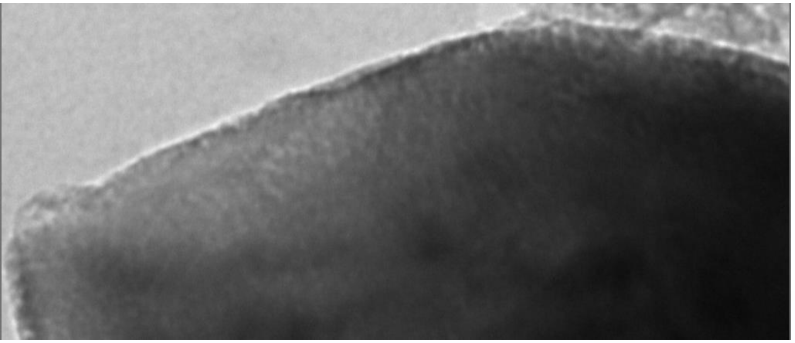
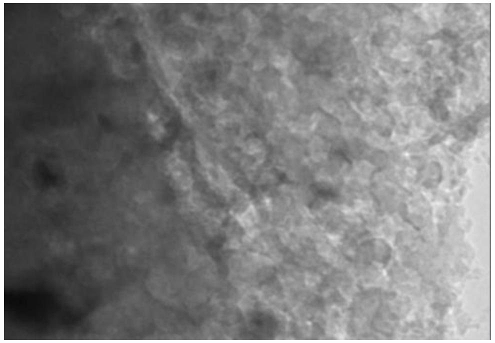
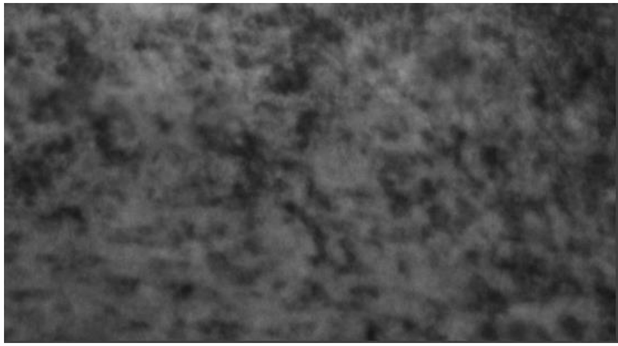

Caitlin A. Taylor, Brittany Muntifering, David Senor, Clark Snow, and Khalid Hattar

September 6th, 2017

Sandia National Laboratories

Bubbles May Affect ^3H Release

- **Bubbles form due to He trapping in lattice defects**

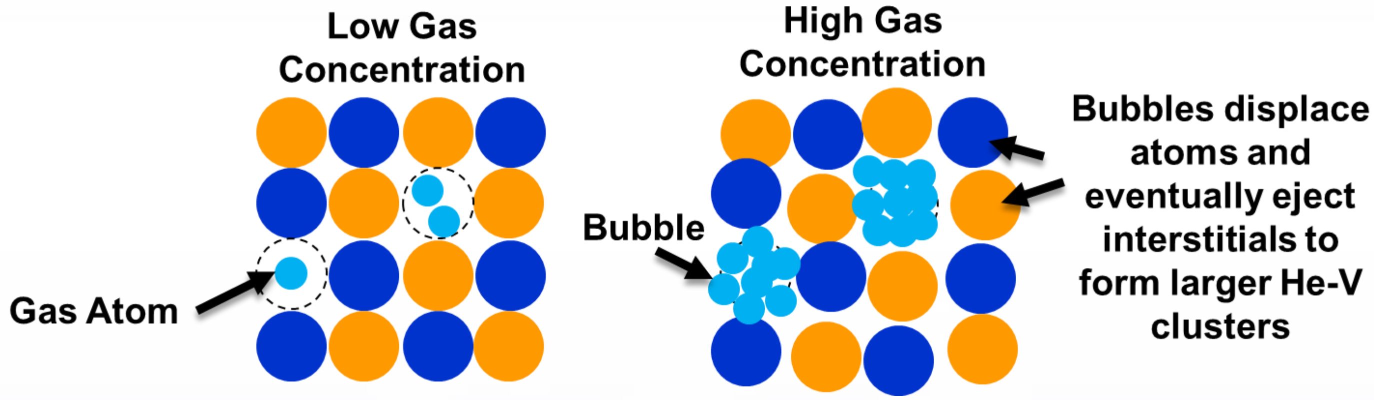

- **Neutron irradiation produces displacement cascades, providing complex defect structures for He or ^3H to trap in.**

MD simulation of displacement cascade in $LiAlO_2$ (PKA = 5 keV)

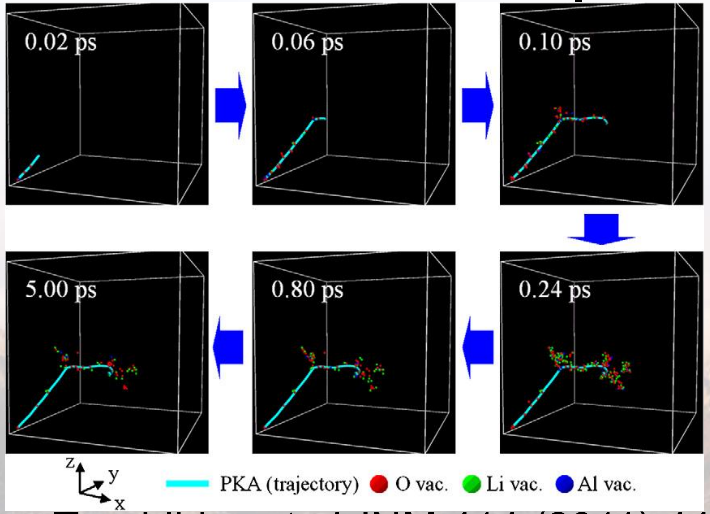

Tsuchihira *et al* JNM 414 (2011) 44-52

Dose Rate Effects

Collaborators: C. Chisholm , P. Hosemann, & A. Minor

7.9 x 10^9 ions/cm^2/s

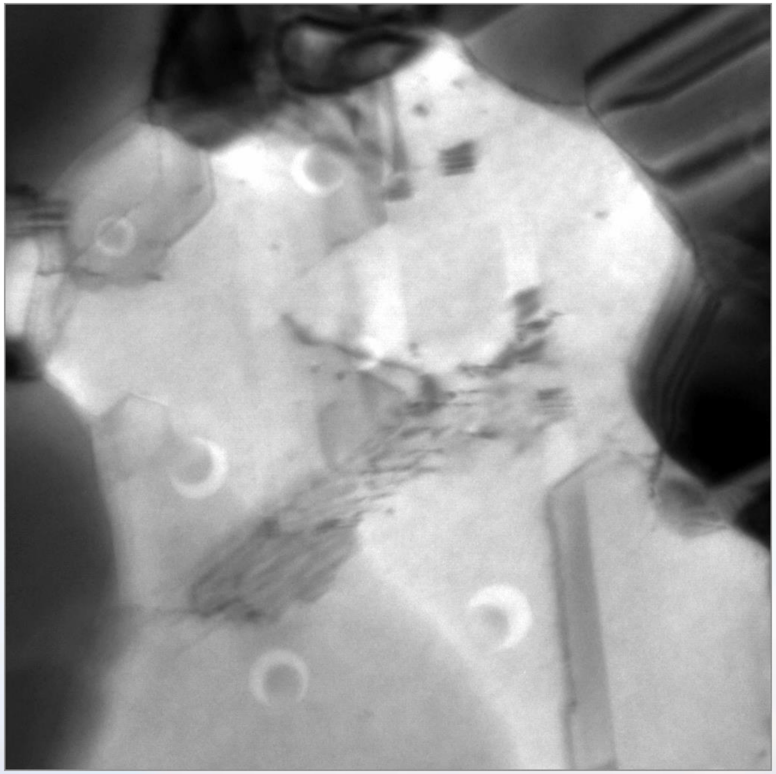

VS

6.7 x 10^7 ions/cm^2/s

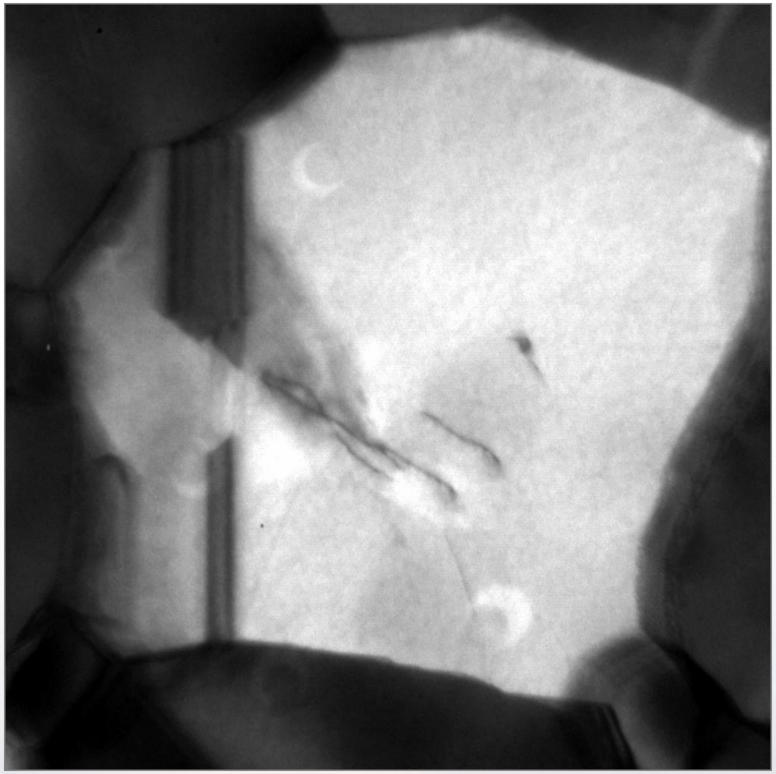

Improved vibrational and ion beam stability permits us to work at 120kx or higher permitting imaging of single cascade events

Simultaneous *In situ* TEM Triple Beam: 2.8 MeV Au^{4+} + 10 keV He^{+}/D_2^{+}

Collaborator: D.C. Bufford

Video playback speed x1.5.

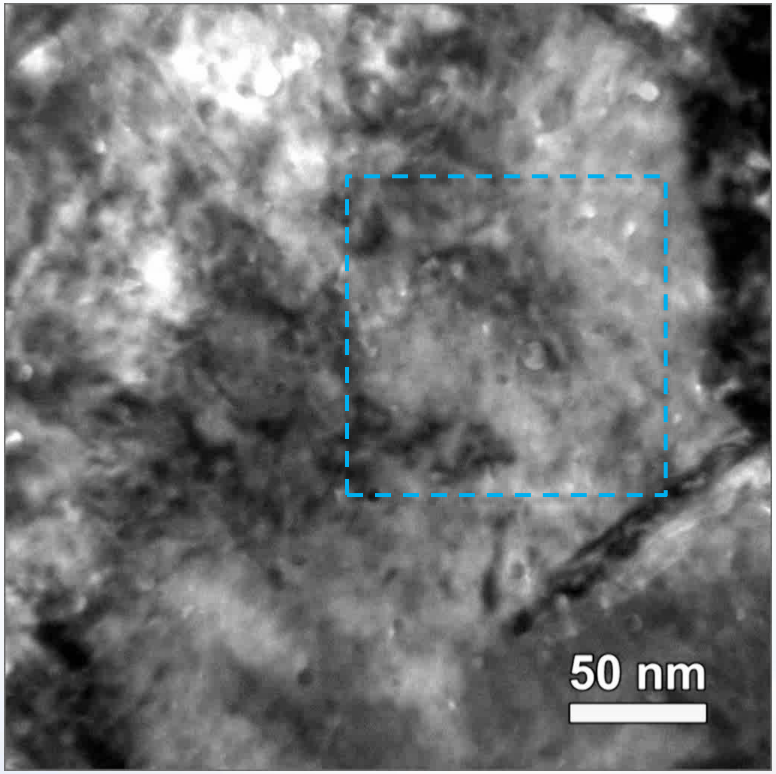

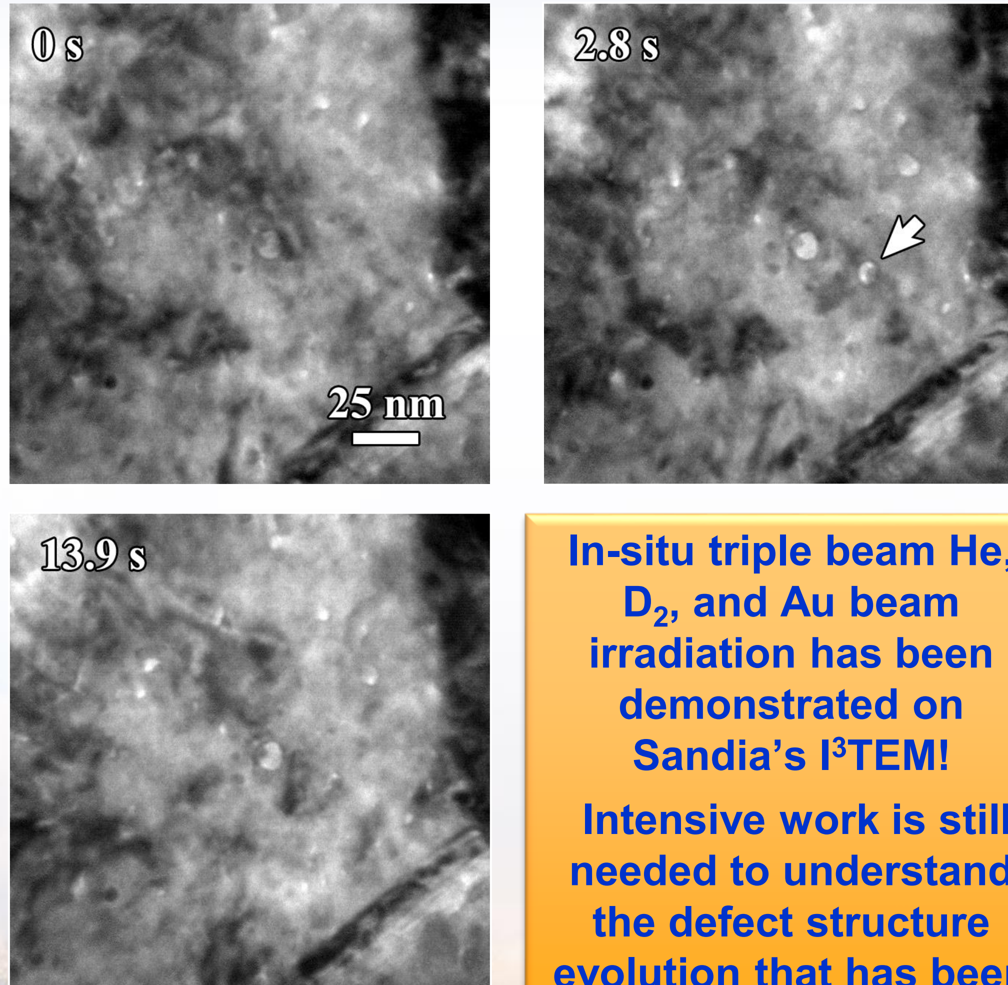

- **Approximate fluence:**
  - Au 1.2 $\times 10^{13}$ ions/cm^2
  - He 1.3 $\times 10^{15}$ ions/cm^2
  - D 2.2 $\times 10^{15}$ ions/cm^2
- **Cavity nucleation and disappearance**

In-situ triple beam He, D_2, and Au beam irradiation has been demonstrated on Sandia's I^{3}TEM!

Intensive work is still needed to understand the defect structure evolution that has been observed.

What Insight into Structural Stability is Gained from I^{3}TEM Experiments?

Collaborators: O. El-Atwani, J. P. Allain, D. Buller, & J.A. Scott

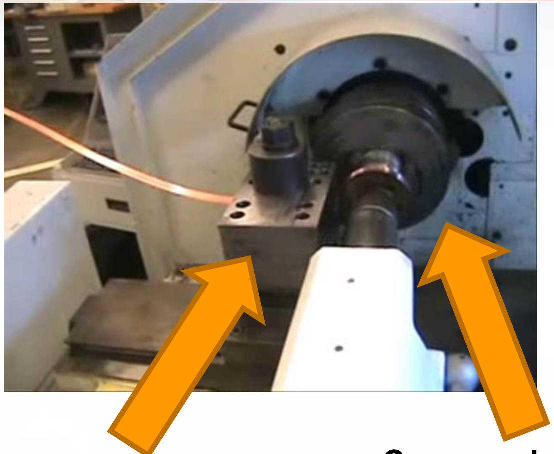

Extrusion Machining tooling

Commercially available lathe

From NW components through proposed NE cladding to waste storage:

Understanding Radiation Damage is Essential

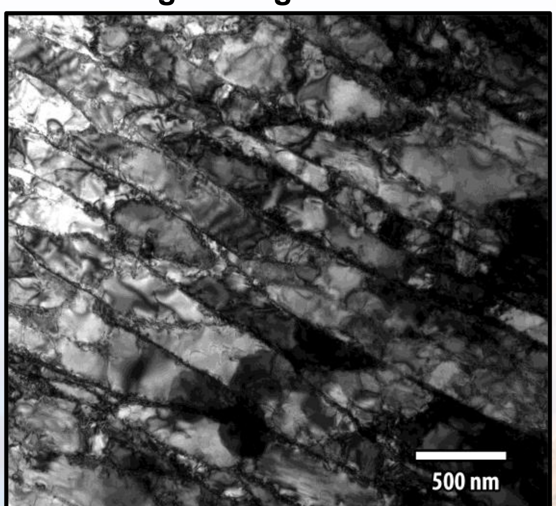

UFG Tungsten

- I^{3}TEM W irradiation and He implantation of SPD-W developed for ITER applications

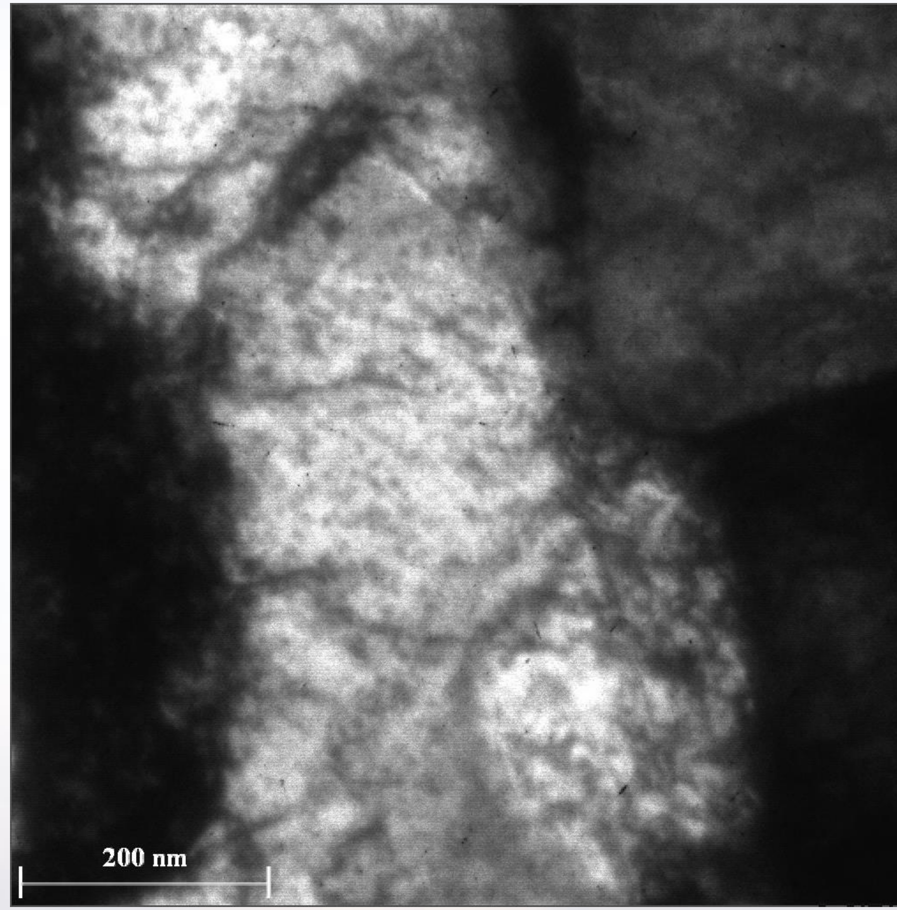

I^{3}TEM is providing insight into:

1) Loop formation
2) Loop stability & migration
3) Rad & structural defect interactions

Scaling down to Nanocrystalline Tungsten Alloys

Collaborators: O.K. Donaldson, T. Kaub, G. Thompson, and J. Trelewicz

Nanocrystalline W

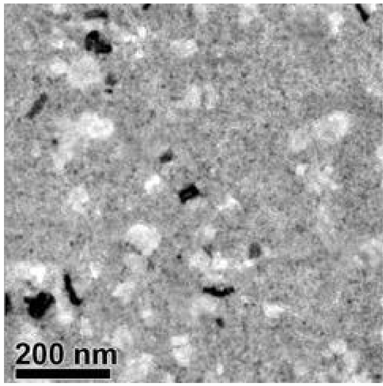

d_{avg} = 30 nm

650 °C →

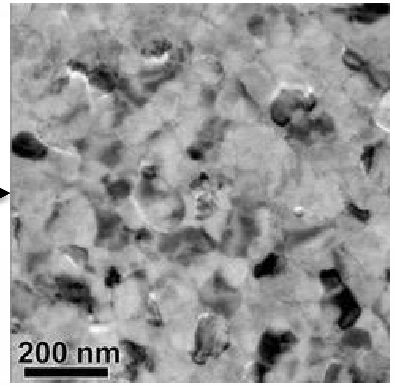

d_{avg} = 86 nm

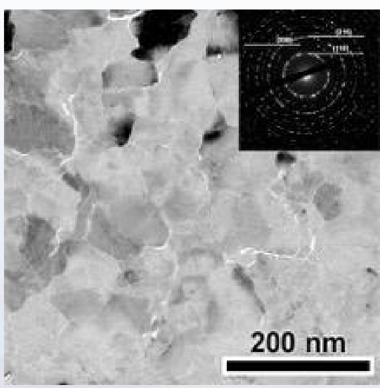

8.5 dpa →

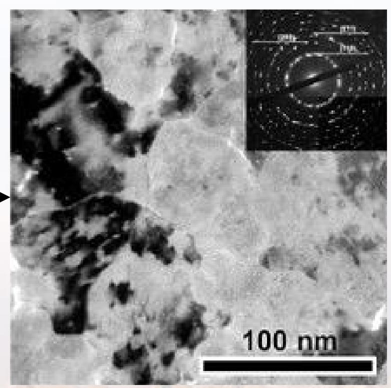

$\rho_{defect} = 2.5 \times 10^{22}\ m^{-3}$

Alloying does not negatively effect radiation tolerance, while improving thermal and mechanical properties

Nanocrystalline W-20at.%Ti

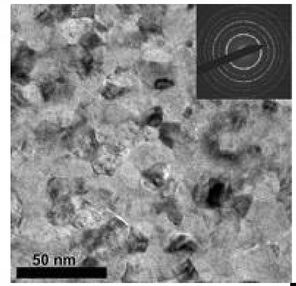

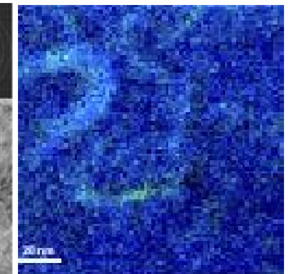

1000° C ↓ Anneal

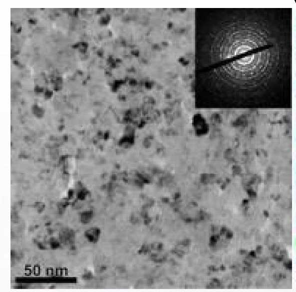

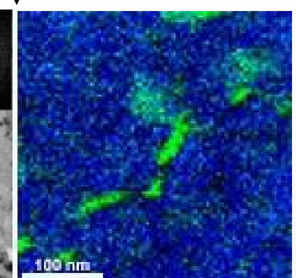

Grain growth is hampered by the addition of Ti

Ti solute is heterogeneously distributed after annealing

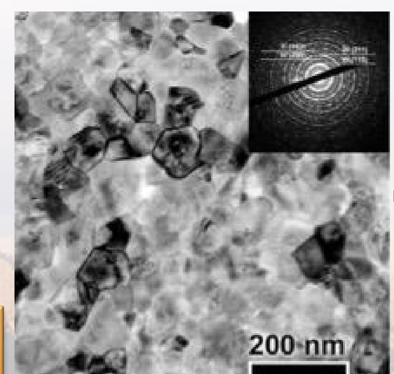

6.3 dpa →

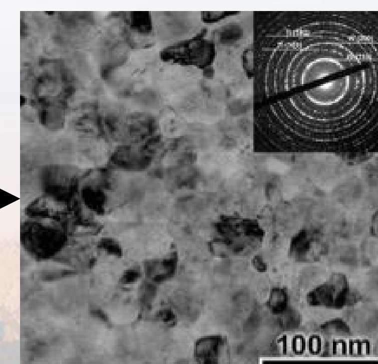

$\rho_{defect} = 2.8 \times 10^{22}\ m^{-3}$

10 keV He^+ Implantation followed by 3 MeV Ni^{3+} Irradiation

Collaborator: B. Muntifering & J. Qu

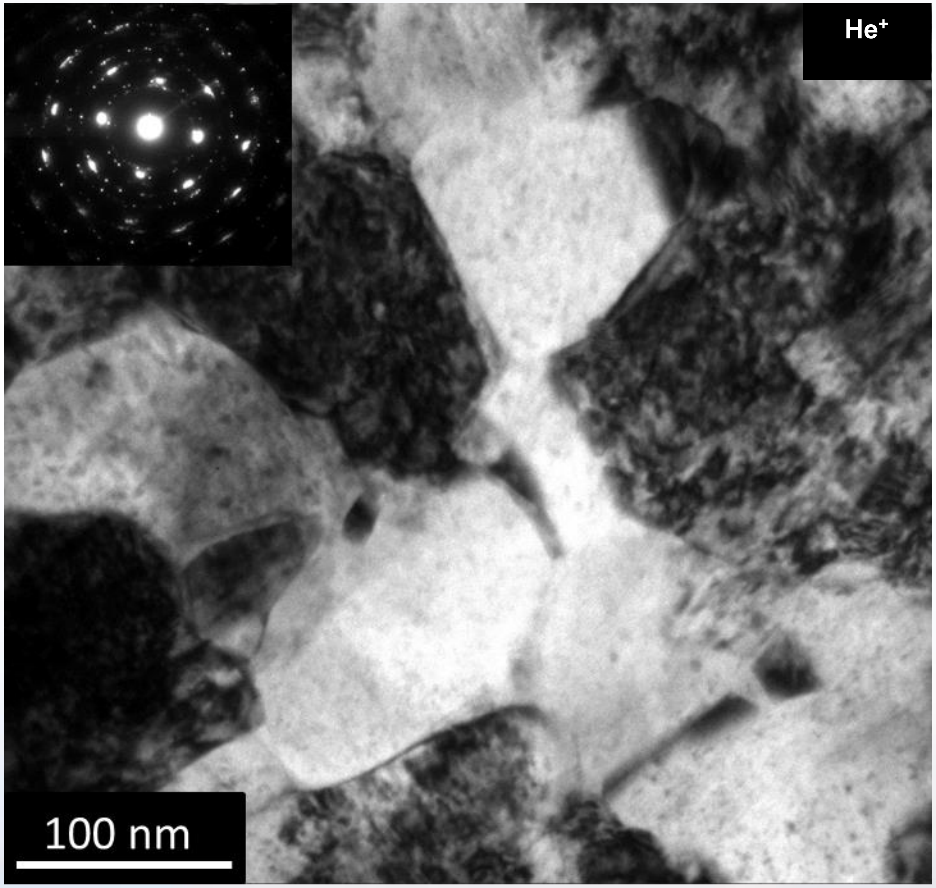

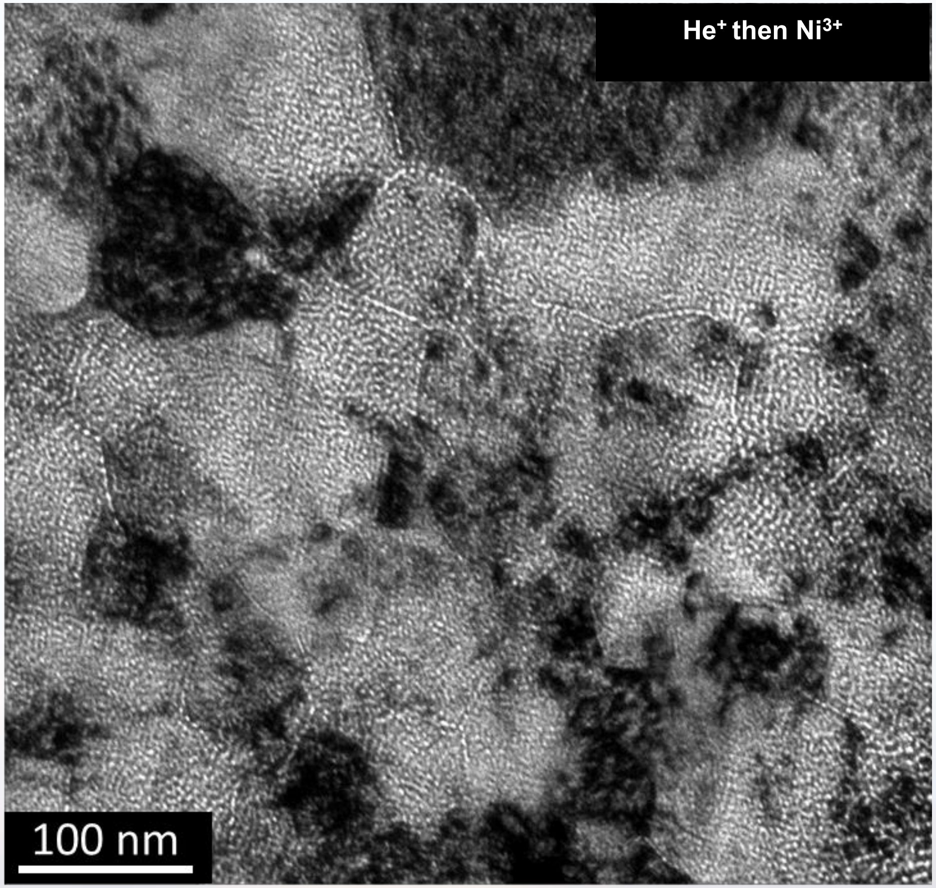

10^{17} He^+/cm^2

Visible damage to the sample

0.7 dpa Ni^{3+} irradiation

High concentration of cavities along grain boundaries

Cavity Growth during In-situ Annealing of 10 keV He^{+} Implanted and then 3 MeV Irradiated Ni^{3+}

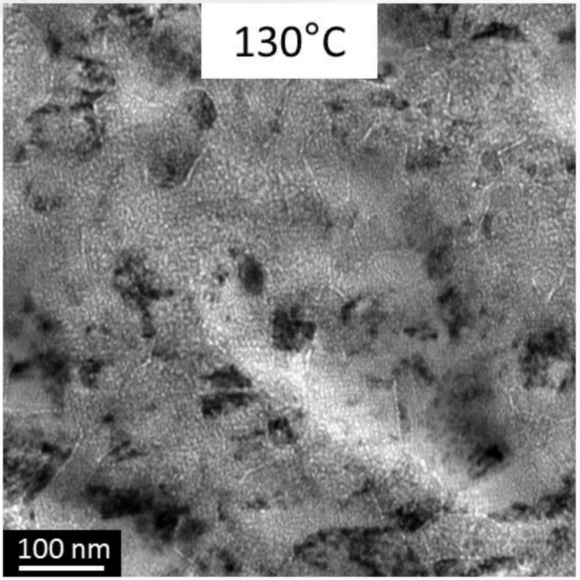

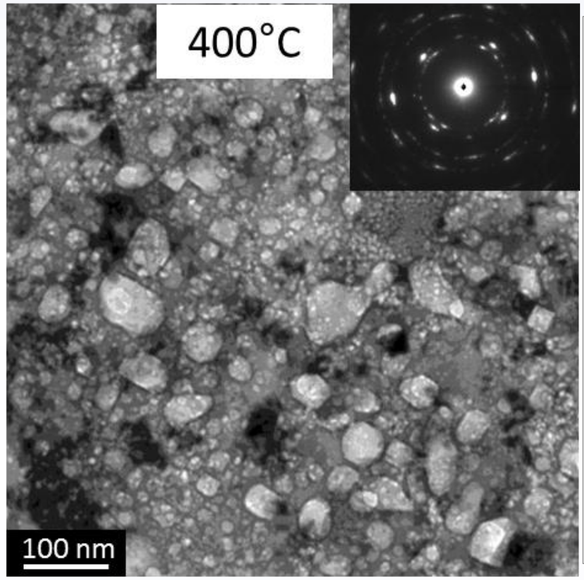

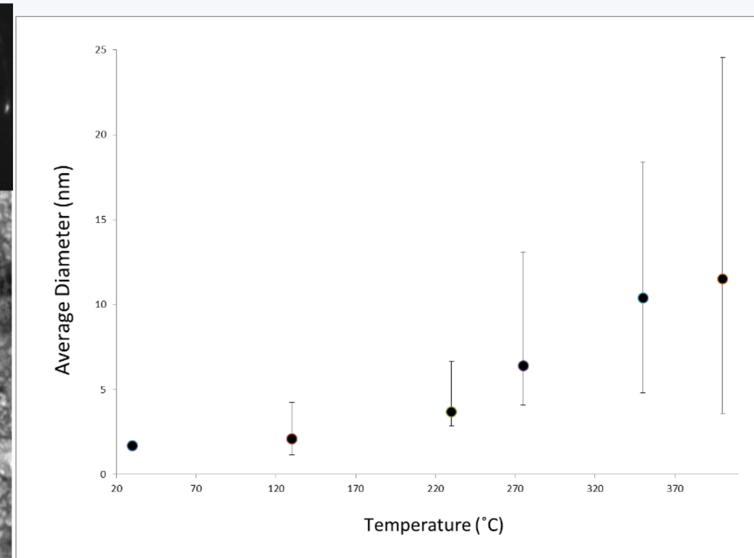

Bubble to cavity transition and cavity evolution can be directly studied

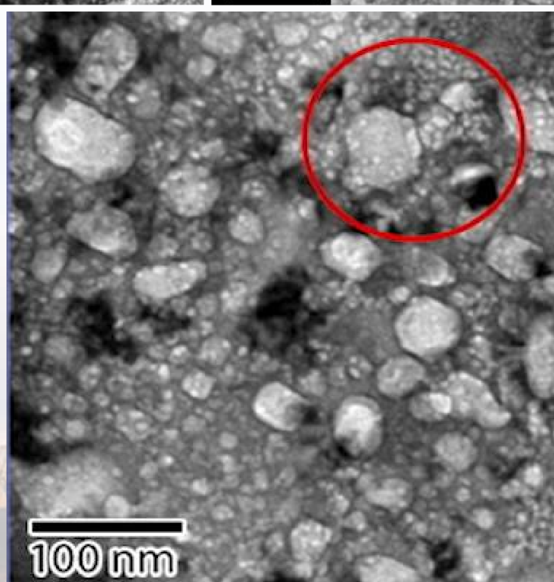

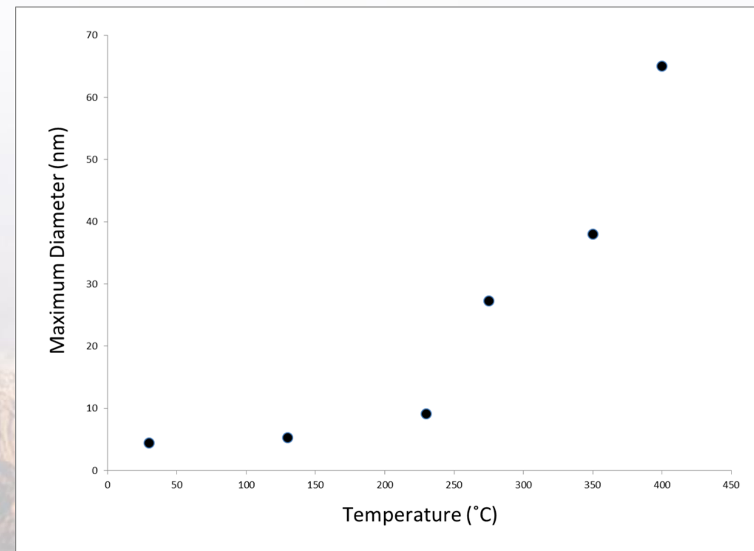

Schematic of the *In situ* SEM Beamline

Collaborators: D.L. Buller & S. Briggs

8/24/2017

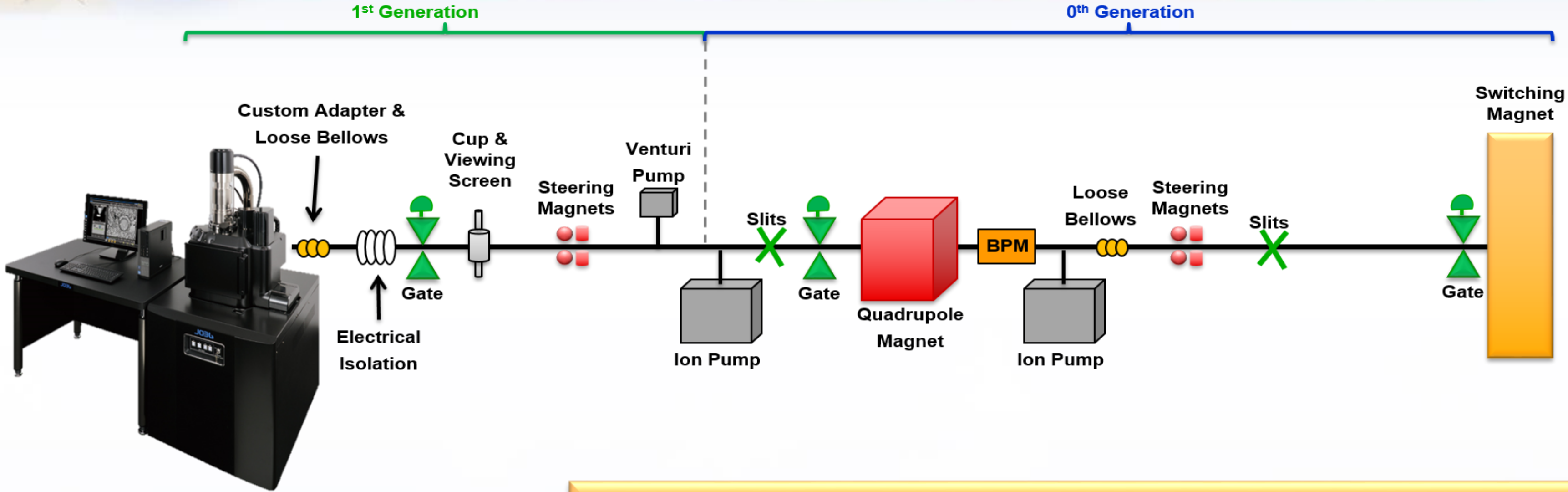

Beam Line planned for the *in situ* SEM will be developed in phases. Ultimate plan is for multiple accelerators being attached for dual or triple beam experiments.

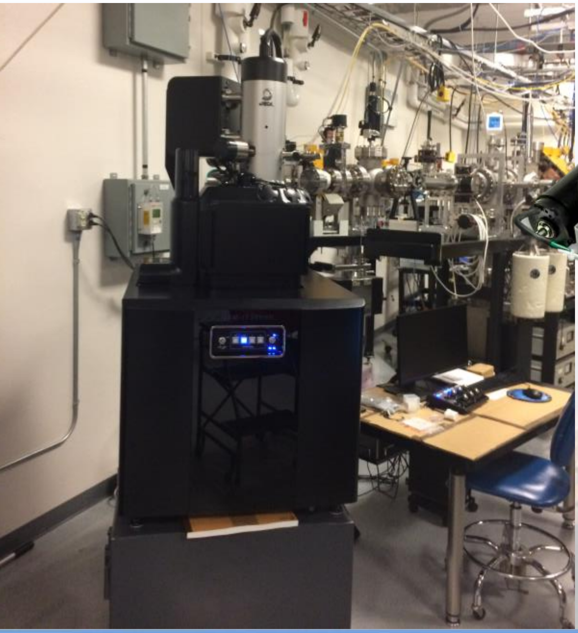

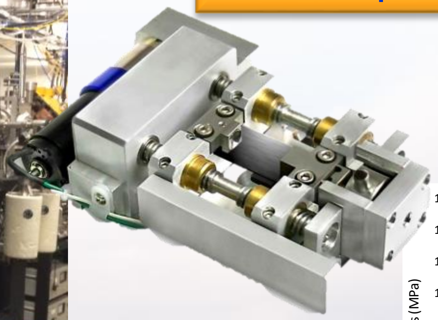

MTI Fullam
Straining Heating

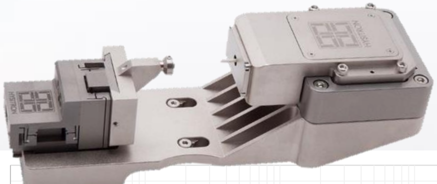

Hysitron PI85
Nanoindenter

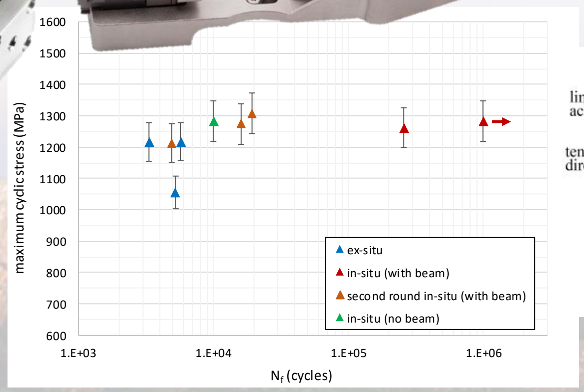

Custom-built Piezo
Fatigue tester

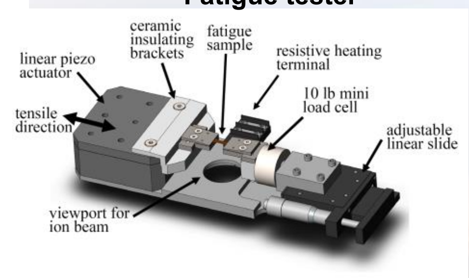

Feasibility of Studying Zircaloy 2 at Nominally 1 atm

Collaborators: S. Rajasekhara and B.G. Clark

Vapor-Phase Heating TEM Stage

- Compatible with a range of gases
- *In situ* resistive heating
- Continuous observation of the reaction channel
- Chamber dimensions are controllable
- Compatible with MS and other analytical tools

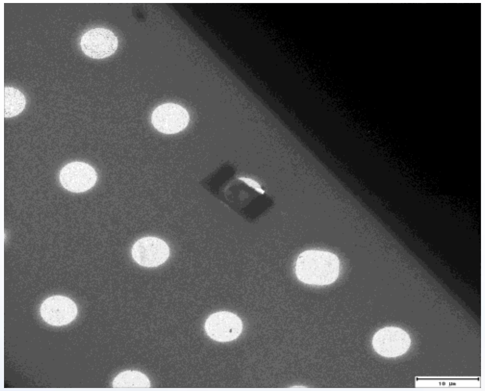

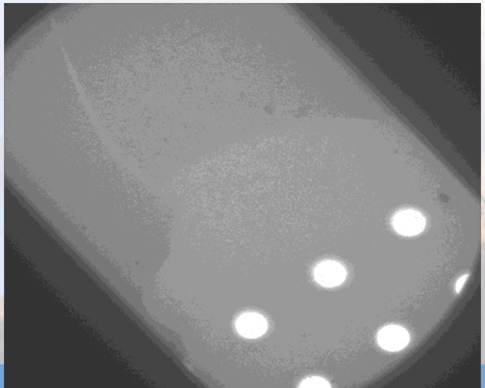

Vacuum & Single Window

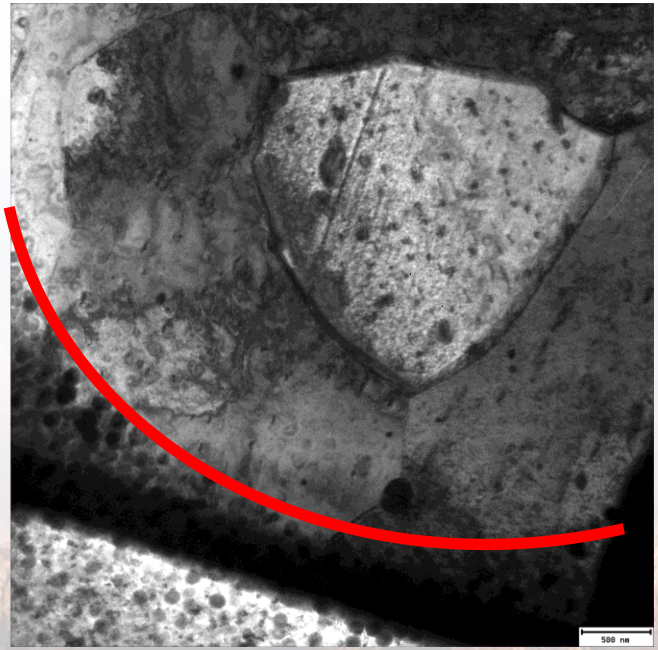

Nominally 1 atm H_2 & Two Windows

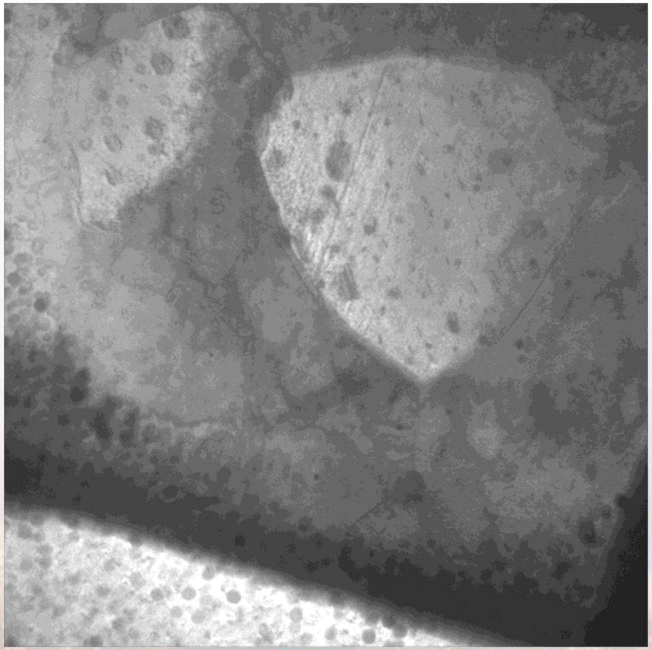

Most features are observed in both despite the decreased resolution resulting from the additional SiN window and 5 µm of air

In situ Observation of Hydride Formation in Zirlo

Collaborators: S. Rajasekhara and B.G. Clark

Absolute hydrogen pressure: 327 torr (~ 0.5 atm),
Ramp rate: 1 ^{o}C/s, Final temperature: ~ 400 C, Dwell time: ~ 90 mins

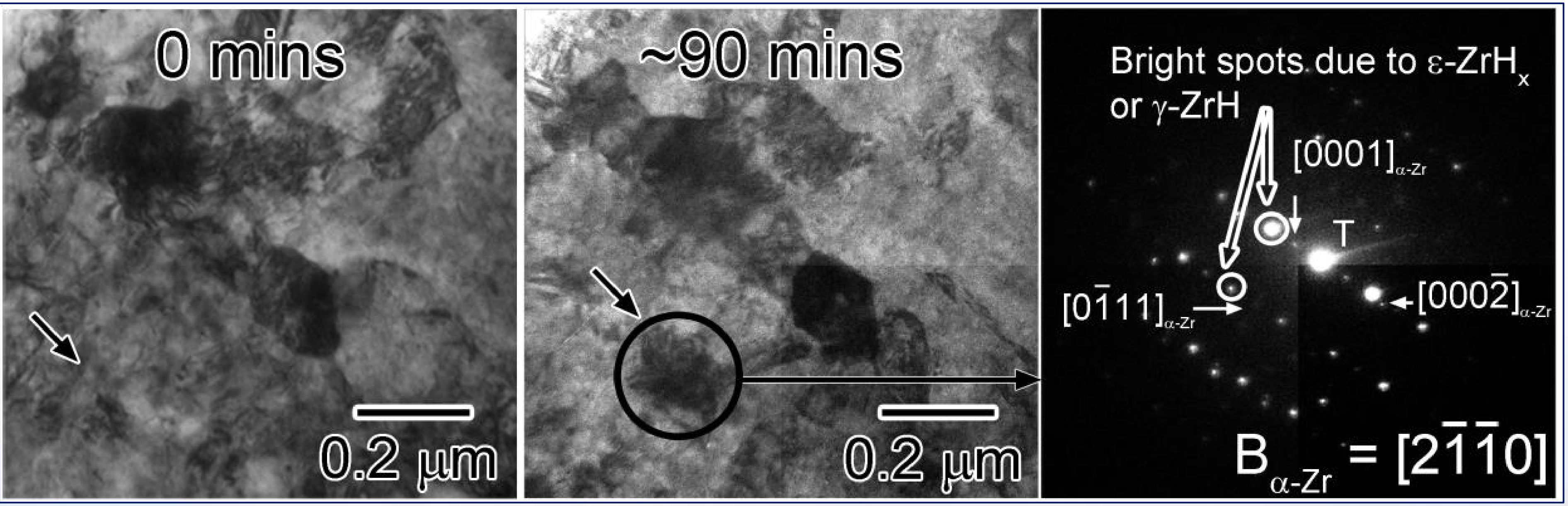

Hydride formation shown, for the first time by use of a novel TEM gas-cell stage, at elevated temperature and hydrogen pressure

In situ Mechanical Testing

Qualitative "Bulk" Mechanical Testing

Minimal control over displacement and no "out-of-box" force information

- **Successful in studies in observing dislocation-GB interactions/mechanisms**
- **Ideally both grains have kinematic BF 2-beam conditions: challenging in ST holder**

Traditional Gatan Heating and Straining Holder

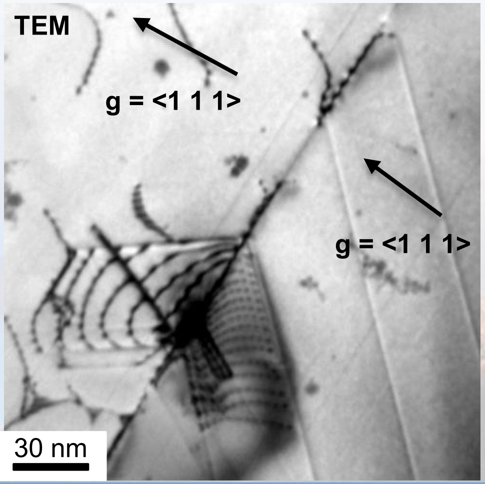

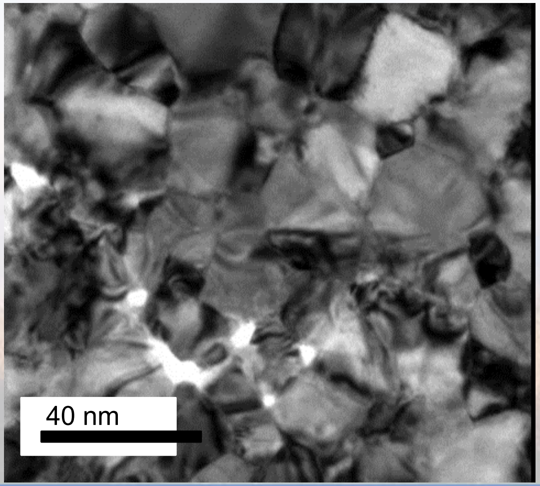

Quantitative Mechanical Testing

Minimal control over displacement and no "out-of-box" force information

- **Sub nanometer displacement resolution**
- **Quantitative force information with μN resolution**

Hysitron PI-95 Holder

1) **Indentation**
2) **Tension**
3) **Fatigue**
4) **Creep**
5) **Compression**
6) **Bend**

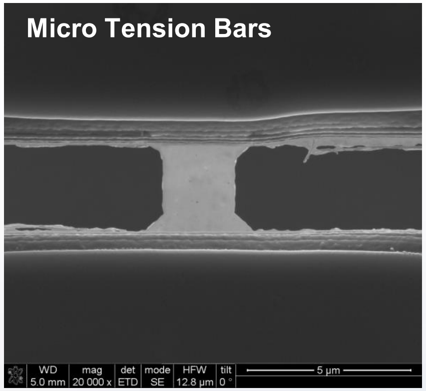

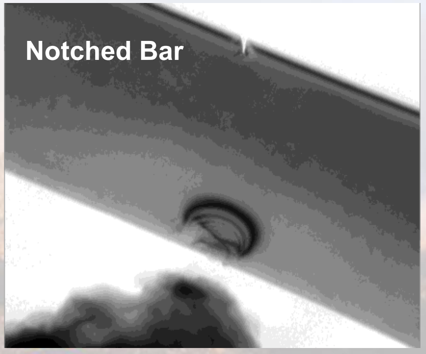

Can We Gain Insight into the Corrosion Process through *In situ* TEM?

Contributors: D. Gross, J. Kacher, I.M. Robertson & Protochips, Inc.

Microfluidic Stage

- Mixing of two or more channels
- Continuous observation of the reaction channel

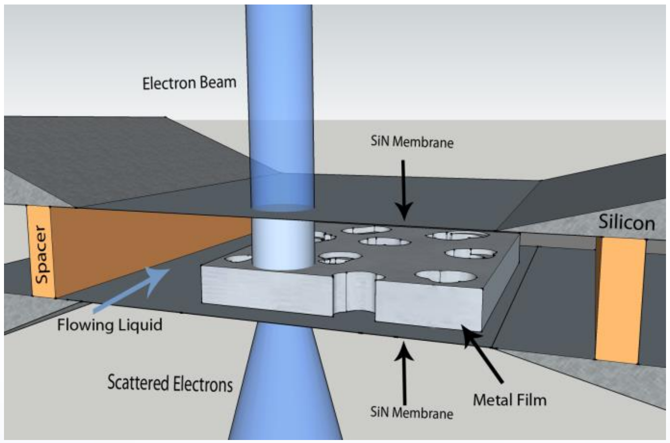

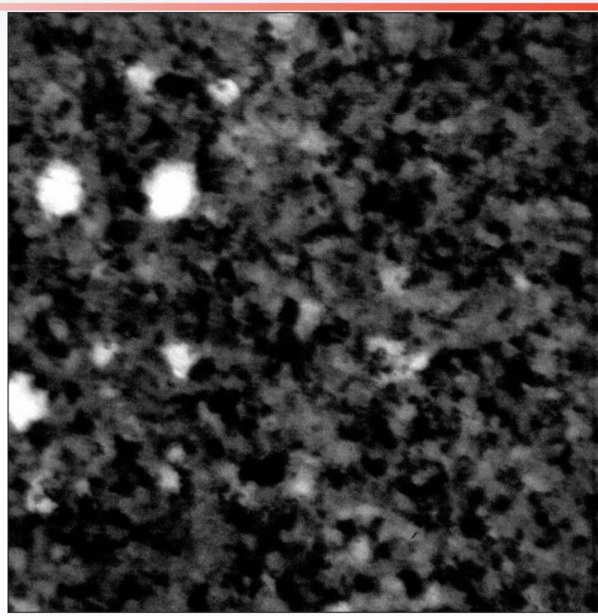

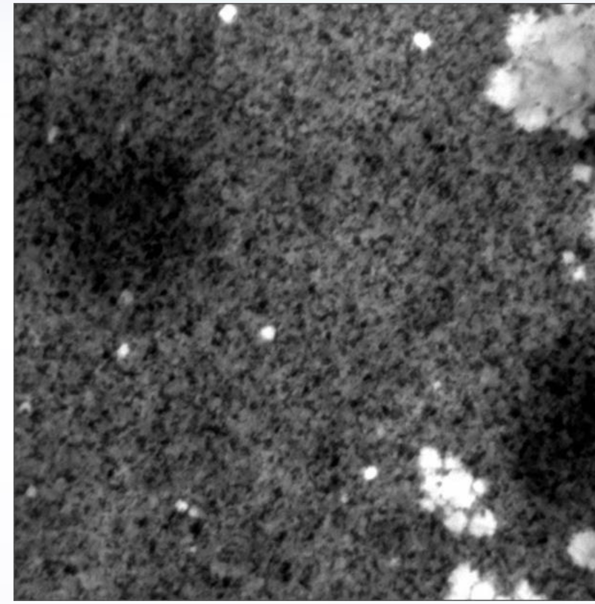

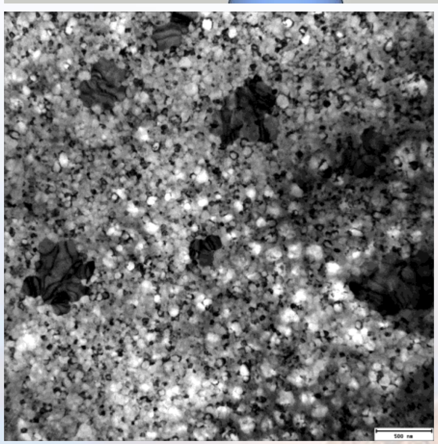

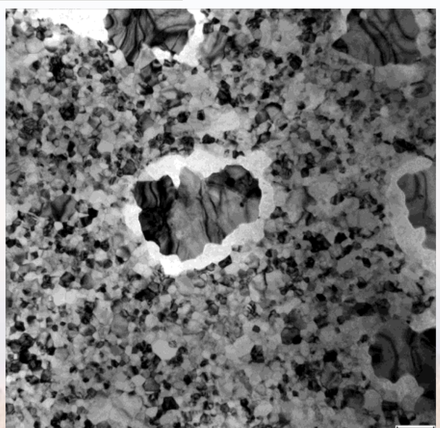

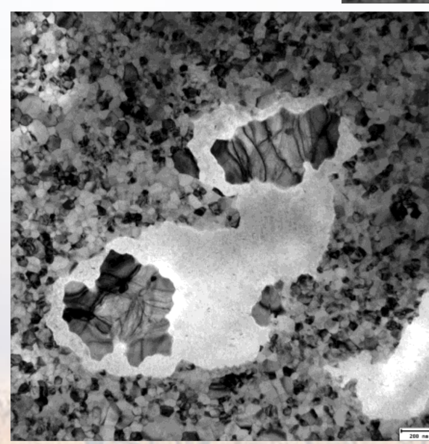

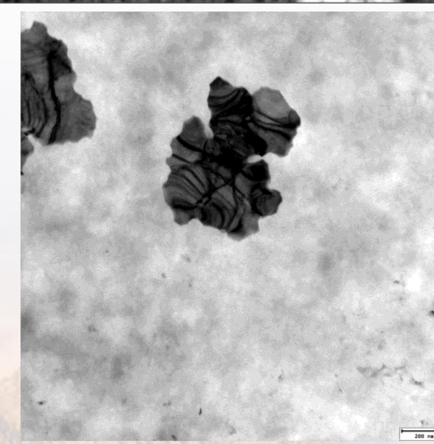

Pitting mechanisms during dilute flow of acetic acid over 99.95% nc-PLD Fe involves many grains.

Large grains resulting from annealing appear more corrosion tolerant